

1069-36891

**NASA TECHNICAL  
MEMORANDUM**

**NASA TM X-53787**

September 26, 1968

NASA TM X-53787

**DEVELOPMENT OF THE MATERIALS DIVISION METEOROID  
SIMULATION FACILITY**

By R. C. Ruff  
Propulsion and Vehicle Engineering Laboratory

**NASA**

*George C. Marshall Space Flight Center  
Marshall Space Flight Center, Alabama*

September 26, 1968

TECHNICAL MEMORANDUM

TM X-53787

DEVELOPMENT OF THE MATERIALS DIVISION METEOROID SIMULATION FACILITY

By

R. C. Ruff

George C. Marshall Space Flight Center  
Marshall Space Flight Center, Alabama

ABSTRACT

An introduction to the meteoroid hazard and the various methods of meteoroid simulation is presented. The Materials Division light gas gun and accessory third stage accelerator hypervelocity launcher is compared to other facilities. A detailed description of the operation and instrumentation of the Materials Division Meteoroid Simulation Facility is presented. The results of firings to date are summarized and the program and simulation capabilities of the facility are discussed.

NASA - GEORGE C. MARSHALL SPACE FLIGHT CENTER

NASA-GEORGE C. MARSHALL SPACE FLIGHT CENTER

---

TECHNICAL MEMORANDUM X- 53787

---

DEVELOPMENT OF THE MATERIALS DIVISION METEOROID SIMULATION FACILITY

By

R. C. Ruff

PROPULSION AND VEHICLE ENGINEERING LABORATORY  
RESEARCH AND DEVELOPMENT OPERATIONS



## TABLE OF CONTENTS

	Page
I. SUMMARY.....	1
II. INTRODUCTION.....	1
III. DESCRIPTION OF FACILITY.....	5
A. Light Gas Gun.....	5
B. Sabot Techniques.....	7
C. Third Stage Accelerators.....	9
D. Range.....	11
IV. INSTRUMENTATION.....	12
A. Piston Velocity Detector.....	12
B. Muzzle Detector.....	13
C. Projectile Velocity Detector.....	14
D. Impact Flash Detector.....	15
E. Crono-Detector.....	15
F. Photographic System.....	15
V. RESULTS.....	16
VI. CAPABILITIES.....	19
VII. CONCLUSIONS.....	20

## LIST OF ILLUSTRATIONS

Table	Title	Page
I.	Summary of Different Types of Hypervelocity Launchers...	22
II.	Summary of Hypervelocity Firings.....	23

# LIST OF ILLUSTRATIONS (Continued)

Figure	Title	Page
1.	Probability Density Function for Meteoroid Air-Entry Velocity.....	26
2.	Mean Impact Flux of Meteoroids With Mass $\geq m$ in Near Earth Orbit.....	27
3.	Materials Division Meteoroid Simulation Facility.....	28
4.	Schematic Diagram of Basic Light Gas Gun.....	29
5.	Polyethylene Piston Before and After Firing.....	30
6.	Schematic Diagram of Sabot Stripper and Gas Separator Tube.....	31
7.	Stripper Pin Assembly, Sabot With Projectile, and Sabot Trap.....	32
8.	Schematic Diagram of Sabot Stripper and Free Flight Separator.....	33
9.	Schematic Diagram of Reduced Area Accelerator.....	34
10.	Schematic Diagram of Constant Area Accelerator.....	35
11.	Schematic Diagram of Tapered Entrance Accelerator.....	36
12.	Range Tank of Meteoroid Simulation Facility.....	37
13.	Schematic Diagram of Range Tank.....	38
14.	Control Room Instrumentation.....	39
15.	Schematic Diagram of Piston Velocity Detector.....	40
16.	Block Diagram of Muzzle Detector.....	41
17.	Block Diagram of The Projectile Velocity Detector.....	42
18.	X-Ray Images of Two Types of Sabot and Projectile Configurations.....	43
19.	Propellant Mass vs. Velocity For Specific Launching Parameters.....	44

# LIST OF ILLUSTRATIONS (Concluded)

Figure	Title	Page
20.	Target Used in Shot 24 Showing Crater and Spall.....	45
21.	Target Used in Shot 11 Showing Circular Symmetry Produced By Bumper Impact.....	46
22.	Target and Bumper Used in Shot 55.....	47
23.	Target and Bumper Used in Shot 50 Indicating Debris Leads Projectile.....	48

## TECHNICAL MEMORANDUM X-53787

### DEVELOPMENT OF THE MATERIALS DIVISION METEOROID SIMULATION FACILITY

#### I. SUMMARY

An introduction to the meteoroid hazard is presented. The various methods used to simulate meteoroid impact are discussed and compared with the capabilities of the Materials Division Meteoroid Simulation Facility. A description of the Meteoroid Simulation Facility is presented. This description includes the basic light gas gun, the sabot stripper, the accessory third stage accelerators, the range tank, and the instrumentation. The results of the firings during the proof and development phase of operation are summarized and discussed. The program capabilities of the Meteoroid Simulation Facility are presented. Simulation of meteoroid impact on specific spacecraft hardware is now in progress.

#### II. INTRODUCTION

Spacecraft designers must anticipate many space environmental factors which can affect the success and usefulness of any given mission. Two of the important factors affecting the operating conditions and the survival probability of a spacecraft are the meteoroid flux and the solar flux of both charged particles and electromagnetic radiation. The effects of the solar flux on the spacecraft are routinely controlled by thermal control coatings and normally are not dependent on the spacecraft size or the length of the mission. The effects of the charged particle radiation are strictly cumulative, so the radiation protection measures need to be increased for longer missions; but the radiation effects normally are independent of spacecraft size. In contrast, the meteoroid environment is much more severe due to the fact that penetration of a spacecraft by even one meteoroid could be catastrophic. For this reason the meteoroid protection measures must be increased for either longer missions or larger spacecraft due to their increased probability of interaction with meteoroids.

To design a spacecraft to a certain safety factor, a designer must have knowledge of the meteoroid environment. The meteoroid environment is described by the meteoroid velocity distribution and the meteoroid mass distribution. It is generally believed that the mass and velocity distributions are fully independent. This implies that any mass range being studied has particles with the same velocity spectrum as all

other mass ranges.

The velocity distribution as gathered from photographic meteor trail data [1] is shown in Figure 1. It can be seen that the velocity extends from 11 km/sec (36,100 ft/sec) to approximately 70 km/sec (230,000 ft/sec). The sharp cut-off at approximately 11 km/sec is due to the velocity increment gained by falling into the earth gravitational field. Meteoroids encountered in interplanetary space could have relative velocities lower than this value. The smaller peak near 65 km/sec (214,000 ft/sec) is still in dispute. Many investigators attribute this peak to instrumental bias and, therefore, try to eliminate it in theoretical calculations. Since all mass ranges have this same velocity distribution, it is often sufficient to simplify calculations by utilizing an average velocity. The average meteoroid velocity recommended for spacecraft design criteria is 26.7 km/sec (87,600 ft/sec) [2].

When these extremely high meteoroid velocities are associated with an impact the term hypervelocity is often used. Hypervelocity is a property of materials and is defined as a speed faster than the speed of sound in the material. For many materials hypervelocity begins at about 5 km/sec (16,400 ft/sec). Above this velocity sound waves can no longer dissipate the energy of impact and shock waves are set up in the materials. The pressures behind the shock waves are sufficiently high to liquefy and vaporize the material which then blows out and disperses leaving a crater.

The mass flux distribution as compiled in Reference 1 is shown in Figure 2. The large mass end of the curve comes from data on photographic meteor trails while the small mass end of the curve is defined by data from the Pegasus spacecrafts and microphone detectors attached to various other spacecraft.

The mass flux distribution can be used to predict the largest meteoroid which can be expected for a given probability of mission success. This is done by dividing the maximum acceptable penetration probability by the product of the spacecraft area, the mission length, and any applicable geometrical factors. The intersection of this threshold flux value and the mass flux distribution defines the largest meteoroid which can be expected to impact the spacecraft during its mission life. The spacecraft must then be designed to withstand impact by a meteoroid of this mass.

A large number of experimental studies of single sheet impact by hypervelocity projectiles have produced a fairly complete set of empirical formulas for predicting penetration of different materials by projectiles of varying density [3]. Unfortunately, these formulas show that the larger meteoroids which can be statistically expected on

extended missions require prohibitively thick walls for the required protection.

A weight saving has been found in the concept of a meteoroid bumper. A meteoroid bumper is an exterior shell of some thickness and composition separated from the spacecraft structural wall by varying spaces of materials and/or vacuum. The effectiveness of any given bumper design depends on several factors. One factor is the degree to which the bumper can break up the meteoroid. It is desirable to vaporize the meteoroid as much as possible. A second factor is the bumper stand-off distance. It is desirable to have as large a stand-off distance as possible to allow the vapor and liquid droplet cloud produced by the meteoroid to spread out over as large an area as possible. A third factor is any layered structure such as thermal insulation which is attached to the spacecraft wall. Because of impedance mismatches, the layered structure can attenuate the shock wave due to the impact of the vapor and liquid droplet cloud and, thereby, make the bumper more effective. The very large number of variables in bumper configurations make it doubtful if a general bumper theory can be developed. At least for the present, each new bumper and insulation configuration will require testing to determine its effectiveness in protecting a spacecraft from meteoroids. To provide the experimental support required for design activity the Materials Division developed the Meteoroid Simulation Facility.

This need for meteoroid simulation to determine the penetration probability of various spacecraft designs has been recognized for many years. Several approaches have been taken to the problem of accelerating projectiles to hypervelocities. In Table I are shown six types of hypervelocity launchers which are or could be adapted to meteoroid simulation. Also, given in the table are the respective velocity limit and projectile description.

As shown earlier, the ideal velocity range for meteoroid simulation would be from 11 km/sec to 25 km/sec. From Table I it can be seen that shaped charge jets, electrostatic accelerators, and drag accelerators can reach well into this velocity range. The electrostatic and the drag accelerators have been used to simulate the surface erosion of spacecraft by so-called micrometeoroids of microgram sizes and smaller. The projectiles, however, cannot be made large enough to simulate penetration of spacecraft walls.

Although the shaped charge jet hypervelocity launchers have a high velocity, they are not used for meteoroid simulation because the jet of material ejected is in a very elongated cylindrical shape which is not useful as a meteoroid simulator. The exploding foil launchers also have projectiles of very irregular shape making them unsuitable for simulation for the same reason.

The light gas gun and the explosive drive are very similar with respect to the type of projectiles and launching techniques. The difference lies in the mechanism used to produce the high pressure and high temperature gases used to accelerate the projectile. The explosive driver utilizes a detonation directed inwards to compress a gas whereas a light gas gun uses a relatively massive piston to compress a gas. The velocity limit of the explosive drivers has only recently [4] been raised above that for light gas guns. The increased velocity for the explosive driver launchers is due to a development in staging explosions behind a projectile. The explosive driver launchers have not yet been used for meteoroid simulation, although they may be used in the future because of the more accurate simulation possible with a higher velocity. A handicap of the explosive driver launcher is that special facilities and techniques must be developed to handle the large amount of high explosive used in each firing.

The light gas gun is, therefore, the only launcher capable of routinely producing hypervelocity projectiles of variable dimensions, mass, and velocity. However, the maximum velocity reaches only to the lower limit of the velocities of meteoroids which can be expected by a spaceship in earth orbit.

A contract was let to develop a light gas gun, according to Materials Division specifications, to provide meteoroid simulation capable of providing support for design activities. As a part of this contract a third stage accelerator was developed to augment the velocity capabilities of the basic light gas gun.

The light gas gun as supplied by the contractor launches a 0.5 inch diameter projectile. The maximum velocity has not yet been attained but is believed to be above 7.6 km/sec (25,000 ft/sec) for the primary projectile. For meteoroid testing the 0.5 inch polycarbonate projectile would be used as a sabot with a much smaller projectile of interest imbedded in its front face. The sabot is destroyed and dispersed as it emerges from the light gas gun barrel while the projectile is allowed to travel to the target unimpeded.

Two approaches were tried by the contractor in developing a third stage accelerator. The first approach was to use the first or primary projectile to shock compress a gas to a very high pressure. This high pressure and high temperature gas is then used to accelerate a secondary projectile which is much smaller than the primary projectile. Indications were that this approach was limited by energy losses from the very high temperature gasses by radiation [5]. The second approach was to try to simulate an elastic collision between the secondary projectile and the relatively massive primary projectile by using a gas column as the elastic medium. The thought was to avoid confining the gas and, therefore, avoid increasing its temperature to a point where energy

losses become important. The results of this approach showed that in all cases where the secondary projectile emerged intact it had a velocity of 1.5 times that of the primary projectile [6].

These two approaches have produced a method of accelerating projectiles to 9.15 km/sec (30,000 ft/sec) using a basic light gas gun of 7.55 km/sec (25,000 ft/sec) capability. In addition, a method of combining the two approaches has been conceived. It is believed that the combination eliminates problems from each of the accelerators and allows an extension of the velocity range to more than 10.7 km/sec (35,000 ft/sec).

### III. DESCRIPTION OF FACILITY

The Materials Division Meteoroid Simulation Facility is shown in Figure 3. The view is from the breech end of the light gas gun hypervelocity launcher toward the barrel and the range tank.

The description of the facility will be divided into the following four sections: the basic light gas gun, the sabot techniques, the third stage accelerators, and the range tank.

#### A. Light Gas Gun

A schematic diagram of the basic light gas gun is shown in Figure 4. Physically the light gas gun consists of the following sections: the breech, the pump tube, the high pressure section, and the barrel. The breech is 3.5 inches inside diameter and two feet in length. It is designed to withstand 50,000 psi internal pressure. However, during routine testing the propellant is chosen to keep the pressure lower than 20,000 psi. The pump tube is 2.5 inches inside diameter and eight feet long. The pump tube contains hydrogen gas in front of the polyethylene piston (which is shown in its prelaunch position). The high pressure section contains a taper from the pump tube to the 0.5 inch diameter barrel. A metal diaphragm burst disc separates the high pressure section from the barrel. The pressures generated by the hydrogen gas as it is compressed by the piston and by the extrusion pressures as the polyethylene piston is stopped are well beyond the elastic limit of the high pressure section bore. These pressures decrease, however, with the inverse square of the radius of the high pressure section. The high pressure section is 12 inches in outside diameter. This large diameter ensures that there are always several inches of steel which have not been subjected to pressures beyond the elastic limit. This elastic outer area will then force the inside area back to its original shape after the gas pressure is dissipated. The high pressure section is a limiting factor in the performance of the light gas gun. Although the

high pressure section can withstand pressures beyond the normal elastic limit, these pressures cannot be increased indefinitely because horizontal extrusion of the steel will begin to occur.

The barrel is 0.5 inch in inside diameter by seven feet long. The barrel also imposes a limitation on the performance of the gun. The high pressure gases produced in the high pressure section also have very high temperatures. This high temperature gas can erode the barrel wall as it flows down the barrel behind the projectile. This is the main reason why hydrogen is used in the light gas gun instead of helium. Due to basic differences in molecular weight and in the ratio of specific heats, hydrogen gas operates at one-fifth the temperature of helium gas for equivalent performance.

The operation of the light gas gun occurs in the following manner. The propellant is ignited by the application of electrical current to an explosive squib. When the pressure generated by the burning propellant reaches a predetermined value, the piston is released. The propellant accelerates the piston to 2,000 to 2,500 ft/sec. The hydrogen gas, which was loaded into the pump tube before firing is compressed by the advancing piston. When the hydrogen pressure reaches a predetermined value, the metal burst disc opens in a petalling fashion along grooves accurately machined on the disc surface. The released gas then begins to accelerate the projectile which was placed approximately two inches from the burst disc. For best results a constant pressure on the base of the projectile would be ideal. However, the pressure behind the projectile has a tendency to drop as the projectile accelerates. To compensate for this normal decrease, the pressure in the high pressure section must be continuously increased during the course of the acceleration. This is accomplished by the taper in the high pressure section. As the piston extrudes into the taper, the volume of gas gets smaller. Therefore, a fixed amount of forward movement of the piston is much more effective in raising the pressure. This taper has been designed to increase the pressure fast enough to compensate for the decrease in pressure due to expansion into the barrel. The amount of piston extrusion can be seen in Figure 5 which shows a piston before and after a firing. The front surface, which undergoes the most extrusion, actually becomes liquid and occasionally flows into the barrel. The groove machined around the base of the piston provides a method of extracting the piston from the high pressure section after a launch.

There are four main variables which control the performance of a light gas gun. They are the propellant mass, the piston mass, the hydrogen gas pressure, and the projectile mass. The propellant mass has been the controlled variable in firings to date. The propellant mass has been varied between 175 and 300 grams of standard M1 howitzer propellant. The piston mass and the hydrogen gas pressure have been kept

constant at 1,300 grams and 95 psia, respectively. The projectiles have been either two or four gram cylinders of Lexan\*, a polycarbonate.

### B. Sabot Techniques

The 0.5 inch diameter Lexan projectile is not itself of interest in simulating meteoroids. However, a smaller projectile of interest can be accelerated to hypervelocities on the front face of the Lexan projectile. In this situation the Lexan projectile is called a sabot. The contractor was additionally asked to adapt standard sabot techniques to the extremely limited existing range tank. The contractor's design has since been modified as a result of in-house development.

There are several techniques which have been developed over the years for separating a projectile from its sabot. Four of these techniques are: (1) petalling-type air-opening sabot; (2) gas separator tube with deflection ramp; (3) spinning segmented sabot; and (4) sabot stripper. Previously, all of these techniques have been used in long dump tanks in which the sabot fragments are allowed to disperse over a long distance and then are trapped while the projectile goes through a hole in the center of the trap and reaches the target. Only the sabot stripping technique was considered capable of being adapted for use in the existing (2-foot long) dump tank.

Figure 6 shows a schematic diagram of the sabot stripper and its associated gas separator tube as delivered by the contractor. The sabot and projectile are seen approaching the end of the light gas gun barrel. The gas separator or compression tube is filled with helium gas at 90 psia contained by two Mylar\*\* diaphragms which are 0.001 inch thick. The stripper consists of four diametrically opposed tungsten pins and is attached to the end of the gas separator.

After penetrating the first Mylar diaphragm, the sabot will experience a very strong retarding force generated by the gas which has been shock compressed to a very high pressure by the hypervelocity impact. The projectile does not see this force, however, because it is totally immersed in the high pressure gas and sees no resultant force. Therefore, the projectile should move past the stripper pins before the decelerating sabot reaches them. This separation is for the purpose of protecting the projectile from the damaging shock waves set up in the sabot upon impact with the stripper pins. These shock waves completely override the mechanical strength of both the sabot and the stripper pins so that there is no longer any effective cohesive bonding. This shocked, highly pressurized cloud of sabot debris will then expand in a radial direction away from the line of flight of the projectile. This expanding cloud is stopped by the sabot trap which is two feet downrange.

Figure 7 is a photograph of a 0.5 inch diameter Lexan sabot.

\* Product of General Electric Company

\*\* Product of E. I. duPont de Nemours and Company

carrying a 1/8-inch diameter aluminum projectile, a sabot stripper pin holder before a launch, and a sabot trap after a launch. The lines in the debris pattern on the sabot trap correspond to the position of the tungsten pins before the launch.

The stripper with gas separator as designed by the contractor has been used on 16 in-house shots with aluminum projectiles. The results have been very inconsistent. In seven of the shots the projectile was off axis and was stopped by the sabot trap. In the remaining shots for which a velocity could be calculated the velocities for identical propellant loading varied widely. In addition, only one of the projectiles emerged without being deformed. The conclusion was reached that the projectile was not separating from the sabot with the result that the projectile was also being decelerated and subjected to a strong shock as the sabot impacted the pins.

When the conclusion was reached that the gas separator did not perform separation, the results of several earlier test shots were again analyzed. The test shots consisted of projectiles in sabots but no gas separators or strippers were used. The X-ray images showed that separation took place even without a gas separator. The mechanism of separation in the test shots was postulated to be as follows: during the launch the sabot is highly compressed by the acceleration. When the sabot emerges from the barrel, the acceleration force is removed and the sabot expands to relieve the compression. It is believed that the expansion and subsequent unconstrained oscillations are sufficient to separate the projectile from the sabot.

To make use of this natural separation the sabot stripper attachment was redesigned. The new design is termed a free flight separator and is shown in Figure 8. In place of the compression tube used in the gas separator the free flight separator has a tube with a bore of 5/8 inch diameter which is larger than the bore of the barrel. This tube allows the sabot to travel approximately 12 inches before it impacts the stripper pins.

Results have shown that use of the free flight separator has directly solved the problem of velocity variation. The velocity is now predictable from the light gas gun loading conditions and is no longer dependent on variables associated with the gas separator tube. In addition, the elimination of the gas separator tube variables has made it possible to study the interaction between the sabot and projectile. For instance, it was discovered that the aluminum projectiles being used were definitely extruding unless fully cradled in a spherical seat.

Another problem with the sabot stripping mechanism which has not been mentioned is the sabot debris which may follow the projectile to the target. The degree of dispersion of the sabot debris is strongly

dependent on the shape of the stripper pins and the pin interference. Research is continuing to improve the dispersion in an effort to completely eliminate the debris which may go through the projectile hole in the sabot trap and impact the target. However, the debris which reaches the target with the present design is so finely dispersed that it normally cannot produce sufficient damage on the target to be confused with the damage from the projectile.

### C. Third Stage Accelerators

The term "third stage accelerator" is applied to the accessory launching assembly which bolts onto the muzzle of the light gas gun. For comparison, the first stage of the series is defined as the acceleration of the piston by the burning propellant and the second stage is defined as the acceleration of the primary projectile by the compressed gas in the high pressure section. The third stage accelerators are designed to accelerate a relatively light secondary projectile by utilizing the kinetic energy of the primary projectile.

Two concepts for a third stage accelerator were developed and tested under the development contract [5, 6]. Figure 9 is a schematic diagram of the first concept. This is called a reduced area accelerator because the secondary projectile is launched down a tube with a smaller diameter than the barrel of the light gas gun. A gas such as helium is contained in the compression tube by a Mylar diaphragm at the barrel end and the secondary projectile at the other end. As the primary projectile breaks the diaphragm and enters the compression tube, it raises the gas pressure which releases the projectile and accelerates it. The difference between this concept and the principle used in the second stage of the light gas gun is that the primary projectile is traveling faster than the speed of sound in the gas which it is compressing. Therefore, the primary projectile produces a shock wave and the secondary projectile is subjected to a very strong pressure pulse. In addition, the shock wave will reflect off the secondary projectile, go back to reflect off the primary projectile, and travel forward again as an even stronger second pressure pulse. The conditions can be set up so that the secondary projectile is still in the launch tube when the second and even third shock waves reach it.

It was found that intact projectiles could be launched with this reduced area accelerator up to a velocity of approximately 8.85 km/sec (29,000 ft/sec). This limitation was believed to be due to the energy losses which become important at the tremendously high pressures and temperatures which are generated after two or three shock compressions. It should be noted that all tests were made with a 1/16-inch diameter launch tube except for two tests with a 3/16-inch diameter launch tube.

The study of the reduced area accelerator is continuing in-house.

It is believed that further testing will determine an optimum diameter for the launch tube. Shots to date have experimented with various types of projectile release mechanisms and with projectile dimensional tolerances with respect to the launch tube diameter.

In an effort to circumvent the energy losses associated with the reduced area accelerator, the second concept was developed. The second concept was that of a constant area accelerator. Figure 10 is a schematic diagram of the constant area accelerator. The description of the operation of this accelerator is the same as that for the reduced area accelerator. The difference lies in the disposition of energy in the compressed gas. In the reduced area accelerator the gas is confined in the compression tube as the kinetic energy of the primary projectile is converted to potential energy in the highly compressed gas. The energy is then reconverted to kinetic energy as the gas expands down the launch tube behind the secondary projectile. In the constant area accelerator the gas acquires kinetic energy immediately since it is not constrained to one volume in space but is allowed to follow the secondary projectile down the launch tube. It would be expected that the elimination of one stage of energy conversion would make the constant area accelerator inherently more efficient than the reduced area accelerator. This was confirmed experimentally. In all valid tests of the constant area accelerator, it was found that the secondary projectile emerged with a velocity of 1.5 times that which the primary projectile had before it entered the compression tube. This indicated that there were no energy limitations entering into the launch cycle up to 9.45 km/sec (31,000 ft/sec) which was the highest velocity which the secondary projectile could acquire without breaking up due to the mechanical stresses during acceleration.

As can be seen in Figure 10, the secondary projectile in the constant area accelerator must be a very thin flat disc for minimum mass compared to the primary projectile. Not only is this a mechanically weak projectile but also it is not a shape which is useful for meteoroid simulation.

The results of these tests combined with the results of experiments on the extrusion of projectiles into reduced area bores [7] led to a method in which it may be possible to reduce the size of the projectile to a more useful shape and still make use of the concept of a constant area accelerator. This combination has been designated the tapered entrance accelerator. Figure 11 shows a schematic diagram of the tapered entrance accelerator.

It has been found [7] that Lexan will extrude into a taper even at hypervelocities. A very useful feature of the extrusion process is that the front face of the projectile actually accelerates and a section will separate when the velocity differential becomes sufficient. It is

believed that this accelerated and separated section of the primary projectile can be used as the driving piston in a constant area accelerator with a bore much less than that of the basic light gas gun. This would allow the projectile to be made much smaller in mass and also to be in a cylindrical shape with a length to diameter ratio close to one. This shape is very strong and also can be useful in meteoroid simulation. It is estimated that with the added advantages of this tapered entrance accelerator the velocity limit will be between 10.6 and 12.2 km/sec (35,000 and 40,000 ft/sec). Experiments to test the concept of the tapered entrance accelerator are planned.

#### D. Range

The range tank of the meteoroid simulation facility can be seen in Figure 12. This view shows the range tank in the right hand side of the picture. The range tank is divided into three sections: the dump tank, the X-ray tank, and the target tank. The impact flash detector can be seen attached to a Plexiglas\* window on the target tank. Also, the three pulse X-ray tubes can be seen attached to an external frame. The three tubes are at 60 degree intervals around the line of flight and each tube has its own long narrow window and its own X-ray film cassette which is introduced through an opening in the bottom of the X-ray tank.

A schematic diagram of the range is shown in Figure 13. The muzzle blast and the sabot debris are contained in the dump tank so that the pressure pulses are kept away from the target as much as possible.

After the projectile leaves the dump tank, it passes through the muzzle detector which produces an electrical trigger pulse when the projectile breaks an infrared beam. The trigger pulse starts a succession of three X-ray pulses as the projectile is traveling over the X-ray film. This information is used for making velocity measurements.

The flash detector on the target tank monitors the light output of the impact. This information is used for making a redundant velocity measurement.

At present the target tank is relatively small as can be seen in Figure 12. The target must physically fit through a 10-inch diameter port and be less than 10 inches deep. An enlarged target tank has been designed and fabricated and will soon be attached to the range.

The new target tank has dimensions of 28 inches deep by 36 inches wide by 48 inches high. The tank door is 27 inches wide by 27 inches high. There are two opposing windows on either side of the projectile line of flight which can be used for photographing the projectile impact.

\* A product of Rohm and Haas Company

A third port in the top of the tank can be used for multiple electrical feedthrus when it is desired to instrument the target. The vacuum system for the new tank is capable of  $10^{-4}$  torr. It will be possible to extend the vacuum capabilities to higher vacuum if it is required for a specific test.

#### IV. INSTRUMENTATION

The firing and control instrumentation is located in the control room adjacent to the room containing the light gas gun and range tank. Figure 14 is a photograph of the instrumentation racks in the control room. Shown in the relay rack on the right from top to bottom is the following instrumentation: a pulsed X-ray control unit, an intercom unit, and an oscilloscope used to display time varying signals such as impact flash. From top to bottom the relay rack at left contains the following: four one-tenth microsecond time interval counters; a switch to close the vacuum valve on the range tank before firing, the firing control panel, and the electrical cable patch panel. Seen on the back wall is the gas loading panel used to charge the pump tube with hydrogen gas prior to firing.

The description of the instrumentation will be broken down into the specific systems and the functions which they perform. The systems which will be described are the following: the piston velocity detector, the muzzle detector, projectile velocity detector, impact flash detector, and crono-detector. In addition a photographic system which is presently on order will be described.

##### A. Piston Velocity Detector

The piston velocity detector is a system for measuring the velocity of the first stage piston just before it enters the high pressure section. This detector is used mainly as a diagnostic tool and is not used on every firing. The measured piston velocity in a given firing gives a more accurate estimate of the velocity of the primary projectile than does the propellant mass. This feature is used for calculating the velocity augmentation when using third stage accelerators since the primary projectile is either destroyed or decelerated. This detector has also been used to determine whether or not a variation in projectile velocity for identical loading conditions is due to some variable in the first stage of acceleration.

A schematic diagram of the piston velocity detector is shown in Figure 15. The three probes for the detector are near the end of the pump tube and are spaced one foot apart. Essentially, the probe is a central wire insulated from a surrounding tube which is at ground

potential. The probe is designed to seal against the pressure which builds up in front of the piston. As the piston travels down the pump tube, it successively will deform each probe so that the central wire is electrically shorted to ground.

When the probe is shorted a capacitor charging current will flow through the gate of a silicon controlled rectifier (SCR). Upon application of the gate signal, the SCR will go from the non-conducting state to the conducting state. Simultaneously, the potential at the cathode of the SCR will drop from the battery voltage to very near ground potential. Since the turn-on time of an SCR is approximately one microsecond, the voltage drop can be considered as a step function when compared to approximately 500 microseconds between probe signals. The battery voltage and dropping resistors are chosen so that sufficient current will flow through the conducting SCR's to keep them in the conducting state indefinitely.

The voltage changes at the cathodes of the SCR's are used to trigger the inputs of two time interval counters. The start input of counter number one is triggered when SCR number one begins to conduct as the piston shorts out probe number one. The counter will count pulses from an internal 10 megahertz clock until it is stopped by a voltage change at the anode of SCR number two. Counter number two will start and stop when the piston shorts out probe numbers two and three, respectively. The time it takes for the piston to travel two successive one foot intervals, therefore, is displayed on the time interval counters in microseconds. The velocity in feet per second is simply calculated as the inverse of the time interval. The velocities of pistons measured to date have ranged from 1,800 to 2,200 feet per second.

This detector was designed for the purpose of solving an immediate problem in projectile velocity variation. The circuit was kept relatively simple to avoid a prolonged detector development delay. The simplicity could be tolerated in this detector because the slow speed of the piston does not require exceptionally high speed circuitry. This detector has now been in use for several months and has been found to be very reliable and simple to use.

#### B. Muzzle Detector

The muzzle detector is a system which detects the passage of the projectile and provides an output trigger for synchronizing other electrical systems. As was shown in Figure 13 the muzzle detector is positioned in the up-range end of the X-ray tank. The projectile must traverse the dump tank and pass through the sabot trap before it reaches the muzzle detector.

A block diagram of the muzzle detector is shown in Figure 16. The

detecting element is a photo-resistive diode on which is focused the light from a GaAs infrared light emitting diode. The muzzle detector is positioned so that the projectile will break the light beam. The photo-resistive diode is chosen so that its speed of response is sufficient to register the passage of a hypervelocity projectile. The resultant voltage change across the photo-resistive diode is amplified and converted to an output pulse capable of triggering other electronic equipment. The output trigger is a positive 45 volt pulse with a rise time of 20 nanoseconds.

The muzzle detector also contains a test modulator which drives the light emitting diode to simulate the passage of a projectile. This provides a means of adjusting the sensitivity of the system to detect projectiles of various diameters and velocities.

### C. Projectile Velocity Detector

The projectile velocity detector is a system for making three consecutive measurements of the projectile position with respect to time. The three measurements give two independent determinations of the projectile velocity. The velocity is calculated as the distance traveled between two measurements divided by the time between the corresponding measurements.

A block diagram of the projectile velocity detector is shown in Figure 17. The three pulsed X-ray units provide the position information while two time interval counters provide the time between X-ray images. The electrical trigger from the muzzle detector is used to simultaneously start the three time delay generators. Each time delay will trigger one of the pulse type X-ray tubes after a preset delay. The delays are set before the shot so that the X-ray pulses will record three successive images of the projectile as it travels down the line of flight. Each X-ray pulse is recorded on individual X-ray film. Each pulse illuminates an area of one inch by 18 inches long. A fiducial line which is the image of a thin wire is common to all three films. The fiducial line is used as a reference for making position measurements.

As each X-ray tube fires, a simultaneous signal is sent to the time interval counters. Each counter measures the time between two successive X-ray pulses. These counters measure down to one tenth of a microsecond. Since it is not expected that the time between pulses will ever be shorter than 10 microseconds, the time interval for the velocity measurements can be considered accurate to one per cent or better. Similarly, the accuracy of the position measurements is kept at approximately one per cent by measuring down to one millimeter and keeping successive images at least 10 centimeters apart. The X-ray pulse is only 70 nanoseconds long which is sufficiently short to eliminate blur due to movement of the projectile. It should be noted that a correction

is made to the position measurements because of parallax between the projectile line of flight and its image on the film which is 6.35 cm away.

Figure 18 is a print of two X-ray negatives showing two types of sabots and projectiles. The stripper pins and sabot trap were not used in these tests.

#### D. Impact Flash Detector

One feature of hypervelocity impact is that a very short but bright flash of light is emitted upon impact. The impact flash detector uses a very high speed photodiode as a sensing element. The output of the photodiode is amplified sufficiently so that the signal can be displayed on an oscilloscope. The oscilloscope is triggered by the muzzle detector. At present the impact flash information is being used mainly for a redundant projectile velocity measurement. However, the impact flash also gives information about the arrival of sabot debris at the target. It can be determined whether there was a large amount of debris and also whether it arrived at the target before or after the projectile.

#### E. Crono-Detector

The crono-detector is another system for a redundant velocity measurement used when another layer of material will not affect the target damage. The sensing element called a crono-card is similar to a capacitor. Two conductive surfaces are applied to a thin insulating sheet and a voltage difference applied. When this sheet is penetrated by the projectile a cloud of ionized gas is formed and a discharge occurs between the two charged surfaces. This discharge pulse is amplified and displayed on an oscilloscope. Two types of crono-cards have been used. One type has closely spaced conductive lines which have been deposited on thin paper while the other type is very thin doubly aluminized Mylar.

#### F. Photographic System

In many cases a dynamic analysis of an impact is of great value in assessing target damage. This is especially true for targets which have more than one layer of material such as meteoroid bumper configurations. For this reason a system capable of making sequential photographs of a hypervelocity impact has been obtained.

The system consists of six imaging devices arranged around a multi-faced prism so that all six images see identical views through a single optical lens. Each imaging device consists of an image converter tube and a Polaroid film holder. An image converter tube operates in the

following manner: when an optical image is focussed on the front face of the tube, a corresponding electron cloud is produced by photo-emission. This electron cloud with a density distribution identical to the original optical image is then accelerated toward the rear face of the tube by a high voltage pulse. When these high energy electrons hit the phosphor-coated rear face, light is emitted in direct proportion to the electron density. This slightly enhanced image is then recorded on Polaroid film.

The usefulness of the image converter is not in the enhancement of the image but in the fact that an image can be produced even with extremely fast high voltage pulses. This system is capable of producing exposures as short as five nanoseconds which is fast enough to stop motion in a hypervelocity impact. In addition to the variable exposure times, the system will have variable interframe delay times ranging from five nanoseconds to 50 microseconds. This makes possible an equivalent framing rate up to 100,000,000 frames per second. The interframe times can be controlled individually to provide a picture sequence which yields the maximum information from a specific projectile and target.

The basic optics of the system produce a 2.5 inch diameter image of a 7-inch diameter object. Accessory close-up optics will provide a 1:1 image to object ratio. The necessary light sources are of high intensity capable of producing the illumination needed for the extremely short exposure times.

With this system it will be possible to analyze the effectiveness of meteoroid bumper configuration in breaking up a projectile and dispersing the debris. In addition the reaction of the target or insulation can be seen.

## V. Results

The primary information from the hypervelocity launches performed during the proof and development phase of operation of the Meteoroid Simulation Facility are summarized in Table II. Included in the table are the following items: the mass of propellant used, the resulting velocity, projectile information, and any special remarks. There have been three major changes in the light gas gun or its operation which should be noted. These are a change in the pump tube loading gas, a change in barrel diameter, and a change in projectile mass. The first change was the conversion of the pump tube loading gas from helium to hydrogen. This conversion took place after shot 21 when hydrogen was approved for use in the Meteoroid Simulation Facility. Although the velocity for identical propellant mass was raised slightly by using the lighter gas, the prime reason for the conversion was that hydrogen has a much lower temperature than helium for the same performance. Consequently, there is much less erosion of the metal at the barrel entrance.

The second major change in the light gas gun was the replacement of the old, much used, and previously enlarged 0.63 inch diameter barrel with a new 0.50 inch diameter barrel. This replacement took place after shot 38. The fact that the replacement with a correctly sized barrel did not immediately raise the velocity is not surprising because projectiles of the same mass were being fired. With the 0.63 inch diameter barrel a 4.0 gram projectile had a length to diameter ratio of approximately one while a 4.0 gram projectile in the 0.5 inch diameter barrel had a ratio of approximately two.

The third change in the operation of the light gas gun brought the length to diameter ratio of the projectile back to one. This reduction in length results in a projectile of 2.0 grams. The 2.0 gram sabot was used in all shots after number 44. As it can be seen in Table II, this last change had the greatest effect on the velocity. Velocities of more than 7.0 km/sec (23,000 ft/sec) are now being reached routinely with only 240 grams of propellant.

The firings during this proof and development phase of the operation of the meteoroid simulation facility were devoted to increasing the velocity attainable with the light gas gun and associated third stage accelerator while at the same time producing projectiles which are not damaged during the launch cycle and are of a shape applicable to meteoroid simulation. Shown in Figure 19 is a graph of velocity versus propellant mass for the different firing conditions. Curves are shown for the 0.63 inch diameter barrel both with helium and with hydrogen as the driving gas and the 0.50 inch diameter barrel with sabot stripper using both the gas separator and with the free flight separator. Some judgement was used in choosing the points which produced these curves because most of the firings were designed to test new techniques and obviously were not indicative of results which can be expected under optimum conditions. The top curve will be used for predicting projectile velocities for future firings. It should be noted that velocities in excess of 7.65 km/sec (25,000 ft/sec) are expected since the light gas gun has already been fired with 300 grams of propellant (shot 36) and only 240 grams of propellant is needed to produce 7.0 km/sec (23,000 ft/sec) (shot 60).

The sabot stripper technique has been shown in shots 44 through 63 to be useful in yielding small projectiles with velocities up to 7.0 km/sec (23,000 ft/sec). The projectiles used in these tests were 1/8 inch diameter spheres of 1100 series aluminum. It was found that this relatively soft aluminum will extrude under the launch acceleration unless fully cradled in a spherical seat. However, it was found that a deep spherical seat raises the probability of a projectile being forced off the center line and impacting the sabot trap. Future testing will be used to determine the optimum depth of the spherical seat for aluminum projectiles. Stronger materials are not expected

to have this extrusion problem.

The extrusion of the aluminum may have been the cause for the poor results when using the gas separator tube. The projectile tended to have a variable velocity lower than expected and also the projectile quite often was forced off of the center line during the stripping operation. These two facts would be explained if the aluminum extruded into its seat in the sabot and would not separate upon entering the gas separator tube. Future tests with different materials will clarify this point.

Two firings with the constant area accelerator and four firings with the reduced area accelerator were made during this phase. The constant area accelerators used in shots 4 and 6 were supplied by the contractor and fired relatively heavy discs. The reduced area accelerators (shots 17, 18, 21, and 37) were new designs produced in the in-house research program. The attainment of a projectile with a velocity of 7.68 km/sec (25,200 ft/sec) after the third design improvement was encouraging. The development of improved accelerators will be speeded as the problems associated with the basic light gas gun are solved.

Targets of many different kinds have been used to stop the projectile. The prime purpose of the targets has been to yield information on the performance of the light gas gun and the accelerators. There were, however, several shots in which the target yielded interesting results.

Figure 20 shows the target used in shot 24. The target is one inch thick case hardened 4140 steel and the projectile was a four gram cylinder of Lexan travelling a 5.10 km/sec (16,700 ft/sec). The left view shows the crater produced by the projectile and the right view shows the spalled area on the rear face. With the 4 gram Lexan projectile spall occurs at all velocities higher than 4.11 km/sec (13,500 ft/sec).

Figure 21 shows the target used in shot 11. The target is one inch thick steel protected by 0.062 inch thick aluminum bumper at a five inch standoff. The interest here lies in the circular symmetry of the pattern on the target. The projectile was four grams of Lexan and was travelling at 4.31 km/sec (14,100 ft/sec). The deformation of the bumper was not due to the projectile impact but was due to the pressure pulse generated between the bumper and the target by the complete vaporization of four grams of Lexan. This pressure pulse was a feature of all shots in which the large projectile was used.

Figure 22 shows the target used in shot 55 for which the stripper was used. The projectile was a 0.047 gram sphere of aluminum traveling

at 6.75 km/sec (22,100 ft/sec). The 0.012 inch thick aluminum bumper was separated from the aluminum target by 2.5 inches. It can be seen that the bumper broke the projectile into many small droplets and spread these over a relatively large area. The holes in the bumper other than the circular projectile hole are due to sabot debris which got through the sabot trap because of incomplete dispersion. Although the debris can penetrate a bumper it does negligible damage on the target as was seen on several shots in which the projectile was off axis and hit the sabot trap. Research is continuing in an effort to completely eliminate the debris, however, because the debris may introduce complications other than direct damage to the target. Figure 23 shows the bumper and target used in shot 50 in which an unusual effect occurred. The crater in the target is the same as that which would occur if no bumper was there. It is postulated that some sabot debris ahead of the aluminum projectile made a hole in the bumper through which the projectile traveled undamaged.

## VI. CAPABILITIES

The capabilities of the Meteoroid Simulation Facility will be described by summarizing the capabilities of the individual items of apparatus and instrumentation described earlier and by relating these to simulation test programs.

The basic light gas gun has been shown to be extremely versatile both for simple meteoroid simulation and for research in velocity augmentation. The light gas gun is capable of launching projectiles from 1/2 inch in diameter down to 3/32 inch in diameter by using the accessory sabot stripper. There is no evidence of a projectile density limitation although projectiles with high ductility may require special care in launching. The reduced area accelerator will launch cylindrical projectiles with various diameters normally below 0.25 inch. The constant area accelerator will launch flat disc shaped projectiles of 0.5 inch diameter and thickness normally less than 0.05 inch.

After launch, the projectile is detected and photographed on three successive X-ray plates. The three images yield two independent measurements of the projectile velocity which are accurate to approximately two percent. In addition the images can be used to determine whether the projectile has been damaged or deformed.

A photographic system is able to give six sequential photographs of an impact process with a variable framing rate up to 100,000,000 frames per second and variable exposure times down to five nanoseconds. This system also is capable of studying the target reaction after the impact.

The target tank presently being installed will accept targets up to 26 inches deep which will fit through a 27 inch by 27 inch door. Windows on the tank provide for photographing the last 20 inches of the projectile line of flight. If necessary, it is possible to instrument and monitor the target with strain gages, pressure gages, and accelerometers. The vacuum in the target tank is in the  $10^{-4}$  torr range.

This facility is technically capable of performing two shots per eight hour day. This is the minimum time needed to perform the following sequence of steps: prepare and install the projectile, target, X-ray cassettes, and sabot stripper attachment or accelerator; prepare the propellant charge; evacuate the range, gas load the pump tube, and fire the light gas gun; clean the pump tube, barrel and range tank; and develop the X-ray plates.

## VII. CONCLUSIONS

1. The basic light gas gun now in routine operation can propel a 0.5 inch diameter, 2 gram, Lexan projectile to more than 7.65 km/sec (25,000 ft/sec).
2. The reduced area accelerator is capable of launching a small cylindrical projectile at velocities up to 9.85 km/sec (29,000 ft/sec). Research is continuing on this concept to provide projectiles more suitable to a simulation test program.
3. A new projectile release mechanism with improved performance has been developed for use in the reduced area accelerator.
4. The tapered entrance accelerator can launch projectiles of useable size for a simulation test program. Research on this concept is continuing.
5. The sabot stripper and gas separator has been found to be capable of launching small spherical projectiles but with an uncontrolled velocity and a low probability of a successful target impact.
6. The free flight separator for the sabot stripper has removed the velocity fluctuation and significantly improved the probability of a successful target impact. Additionally, the velocity, using this technique, is higher than that of the gas separator.
7. The minimum size projectile recommended for use with the sabot stripper is 3/32 inch in diameter. No projectile density limitation has been found but materials of high ductility such as 1100 series aluminum require special care.

8. The piston velocity detector gives a more accurate measurement of the projectile velocity than is possible from a prediction based on propellant mass. This detector is useful in trouble shooting and also in accelerator shots where the primary projectile is either stopped or slowed.

9. The projectile velocity detector measures velocity to two percent or better accuracy. In addition, the X-ray photographs give information on projectile integrity and geometry in flight.

10. The photographic system is capable of yielding six pictures of the impact process at a variable rate up to 100,000,000 frames per second.

11. The target tank being installed is 28 x 36 x 48 inches in size and will be evacuated down to  $10^{-4}$  torr. The tank will accept any target which will fit through a 27 x 27 inch door and is less than 26 inches long.

12. The Materials Division Meteoroid Simulation Facility is technically capable of performing two hypervelocity firings per eight hour day.

TABLE I

SUMMARY OF DIFFERENT TYPES OF HYPERVELOCITY LAUNCHERS

<u>Hypervelocity Launchers</u>	<u>Maximum km/sec</u>	<u>Velocity ft/sec</u>	<u>Projectile Description</u>
Light Gas Guns	9.15	30,000	Single discrete projectile, 1/16 inch diameter and up
Explosive Driver	12.2	40,000	Single discrete projectile, 1/16 inch diameter and up
Exploding Foil	9.15	30,000	Plastic, large diameter to thickness ratio
Shaped Charge Jets	15.2	50,000	Random mass, small diameter to thickness ratio
Electrostatic Accelerator	15.2	50,000	Multiple, microgram projectile
Drag Accelerator	15.2	50,000	Multiple, microgram projectile

TABLE II SUMMARY OF HYPERVELOCITY FIRINGS

SHOT NO.	DATE	PROP. MASS (GR)	PROJECTILE		REMARKS
			VELOCITY (KM/SEC)	SHAPE	
1967					
1	6-13	175	4.08	13,400	Constant area accelerator
2	6-14	175	4.08	13,400	
3	6-14	175	4.11	13,500	
4	6-15	175	6.16	20,200	Constant area accelerator
5	6-16	200	4.42	14,500	
6	6-16	200	6.86	22,500	
7	6-19	200	4.30	14,100	Projectile deflected
8	6-21	200	-	-	
9	6-23	200	4.33	14,200	
10	7-7	200	4.33	14,200	No X-ray image
11	7-12	200	4.31	14,100	
12	7-14	200	4.33	14,200	
13	7-21	220	4.63	15,200	
14	7-25	220	4.45	14,600	
15	7-27	220	-	-	
16	8-1	220	4.48	14,700	
17	8-7	175	-	-	
18	8-16	200	5.18	17,000	
19	9-12	200	4.30	14,100	
20	9-14	200	3.96	13,000	Reduced area accl., failed Reduced area accl., clean impact Prettrigger on muzzle detector 0.125 inch separation from sabot Reduced area accelerator
21	9-18	200	7.68	25,200	
Conversion from helium to hydrogen gas in pump tube					
22	9-27	200	4.33	14,200	Projectile broke up
23	9-29	220	-	14,200	

TABLE II SUMMARY OF HYPERVELOCITY FIRINGS (Continued)

SHOT NO.	DATE	PROP.		PROJECTILE		SHAPE	MASS (GR)	REMARKS
		MASS (GR)	VELOCITY (KM/SEC)	VELOCITY (FT/SEC)	MAT'L.			
24	10-5	220	5.10	16,700	Lexan	Cyl.	4.00	Pretrigger on muzzle detector
25	10-9	220	4.42	14,500	Lexan	Cyl.	4.00	
26	10-10	230	5.00	16,400	Lexan	Cyl.	4.00	
27	10-16	240	5.22	17,100	Lexan	Cyl.	4.00	
28	10-19	250	-	-	Lexan	Cyl.	4.00	
29	11-8	200	-	-	Lexan	Cyl.	4.00	Gas separator, proj. hit sabot trap
30	11-14	220	4.89	16,100	Lexan	Cyl.	4.00	
31	11-21	240	-	-	Fe	Ball	0.056	
32	11-28	260	5.47	17,900	Al	Ball	0.047	
33	12-5	260	5.26	17,300	Fe	Ball	0.443	
34	12-14	280	5.76	18,900	Fe	Ball	0.443	Pretrigger, no X-ray images
35	12-19	280	-	-	Lexan	Cyl.	4.00	
36	12-26	300	5.60	18,400	Al	Ball	0.047	
1968								
37	1-4	250	-	-	Al	Cyl.	0.090	Reduced area accl., no X-ray
38	1-23	220	-	-	Al	Ball	0.047	Gas separator, no stripper
Conversion from 0.63 to 0.50 inch dia. barrel								
39	2-5	250	-	-	Lexan	Cyl.	4.00	Pretrigger, no X-ray images
40	2-7	260	-	-	Lexan	Cyl.	4.00	Pretrigger, no X-ray images
41	2-8	180	5.10	16,700	Lexan	Cyl.	4.00	Pretrigger, only two X-ray images
42	2-9	200	-	-	Lexan	Cyl.	4.00	Pretrigger, no X-ray images
43	2-15	220	5.00	16,400	Lexan	Cyl.	4.00	Pretrigger, only two X-ray images
44	2-16	240	-	-	Al	Ball	0.047	Pretrigger, only one X-ray image

TABLE II SUMMARY OF HYPERVELOCITY FIRINGS (Concluded)

SHOT NO.	DATE	PROP.		PROJECTILE		MAT'L.	SHAPE	MASS		REMARKS
		MASS (GR)	VELOCITY (KM/SEC)	VELOCITY (FT/SEC)						
Conversion from 4.00 to 2.00 gram sabot										
45	2-26	180	5.23	17,200	Al	Ball	0.047		Gas separator	
46	2-28	200	4.90	16,100	Al	Ball	0.047		Gas separator, proj. flattened	
47	3-4	220	6.33	20,700	Al	Ball	0.047		Gas separator	
48	3-6	240	-	-	Al	Ball	0.047		Gas separator, proj. hit trap	
49	3-11	260	-	-	Al	Ball	0.047		Gas separator, proj. hit a pin	
50	3-14	240	6.58	21,600	Al	Ball	0.047		Gas separator, proj. deformed	
51	3-18	260	-	-	Pb	Ball	0.204		Gas separator, proj. hit trap	
52	3-25	260	6.40	21,000	Pb	Ball	0.204		Gas separator, proj. broken	
53	3-26	240	6.58	21,600	Al	Ball	0.047		Gas separator	
54	4-1	240	6.40	21,000	Pb	Ball	0.204		Gas separator, proj. broken	
55	4-2	260	6.75	22,100	Al	Ball	0.046		Gas separator, proj. broken	
56	4-4	260	7.20	23,600	Al	Ball	0.041		Gas separator, proj. deformed	
57	4-5	240	-	-	Al	Ball	0.041		Gas separator, proj. hit trap	
58	4-9	240	-	-	Al	Ball	0.041		Gas separator, proj. hit trap	
59	4-10	240	6.75	22,100	Al	Ball	0.041		Gas separator, proj. deformed	
60	4-11	240	7.10	23,200	Al	Ball	0.041		Free flight separator	
61	4-15	240	-	-	Al	Ball	0.041		Free flight, proj. hit trap	
62	4-18	240	7.00	23,000	Al	Ball	0.041		Free flight, proj. deformed	
63	4-22	240	6.73	22,300	Al	Ball	0.041		Free flight, proj. deformed	

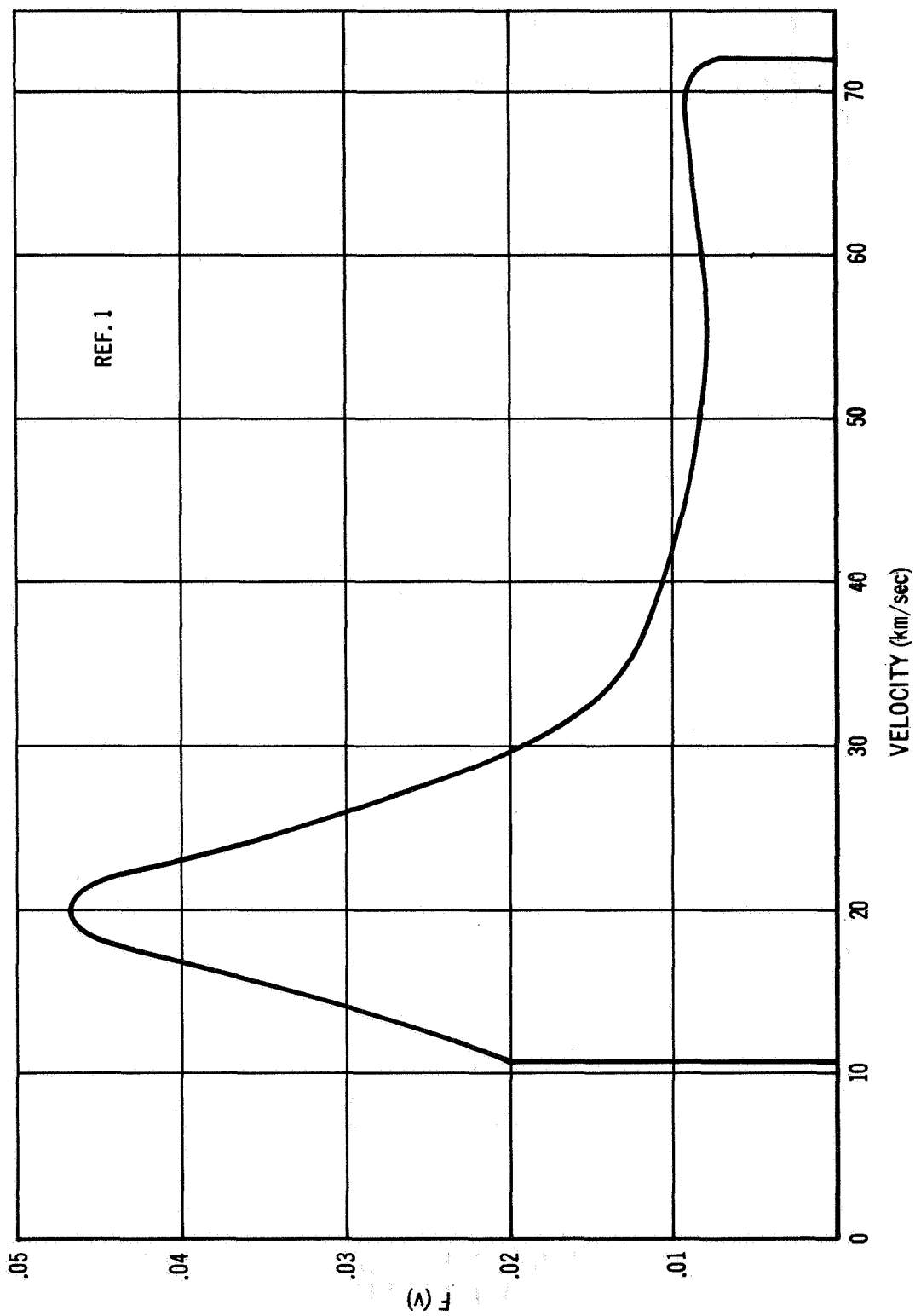


FIGURE 1. PROBABILITY DENSITY FUNCTION FOR  
METEOROID AIR-ENTRY VELOCITY

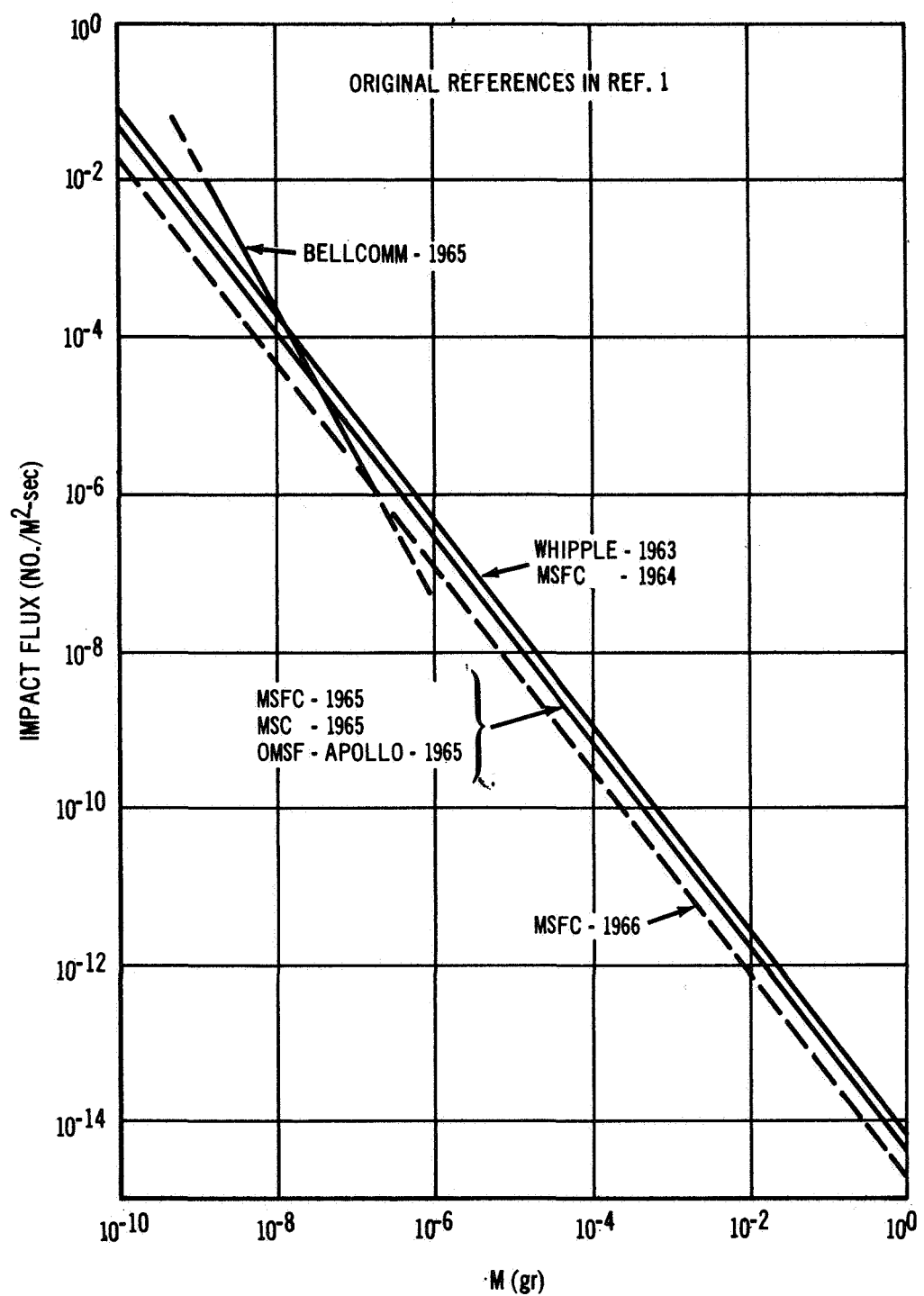


FIGURE 2. MEAN IMPACT FLUX OF METEORIDS WITH MASS  $\geq m$  IN NEAR EARTH ORBIT

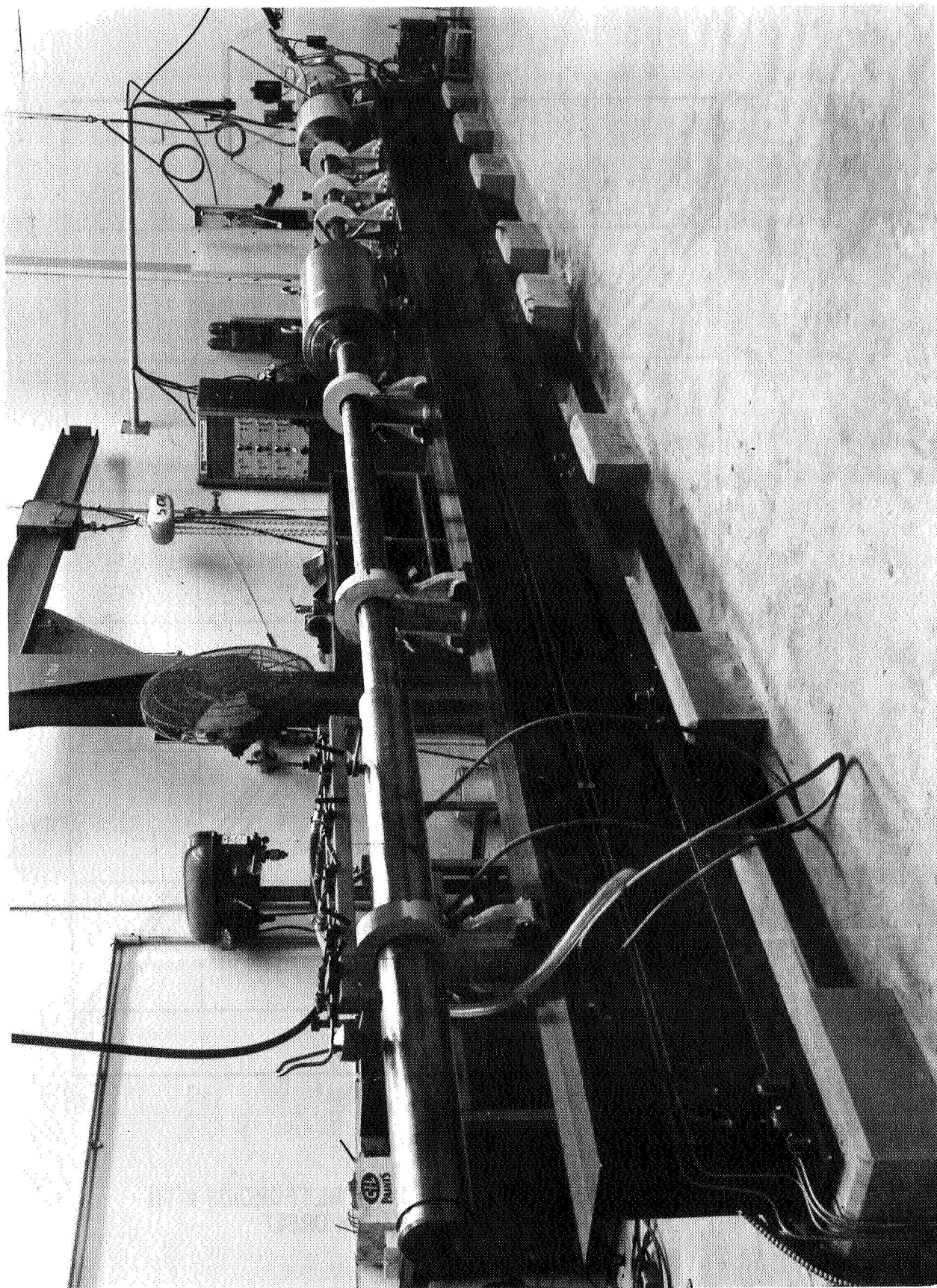


FIGURE 3. MATERIALS DIVISION METEOROID  
SIMULATION FACILITY

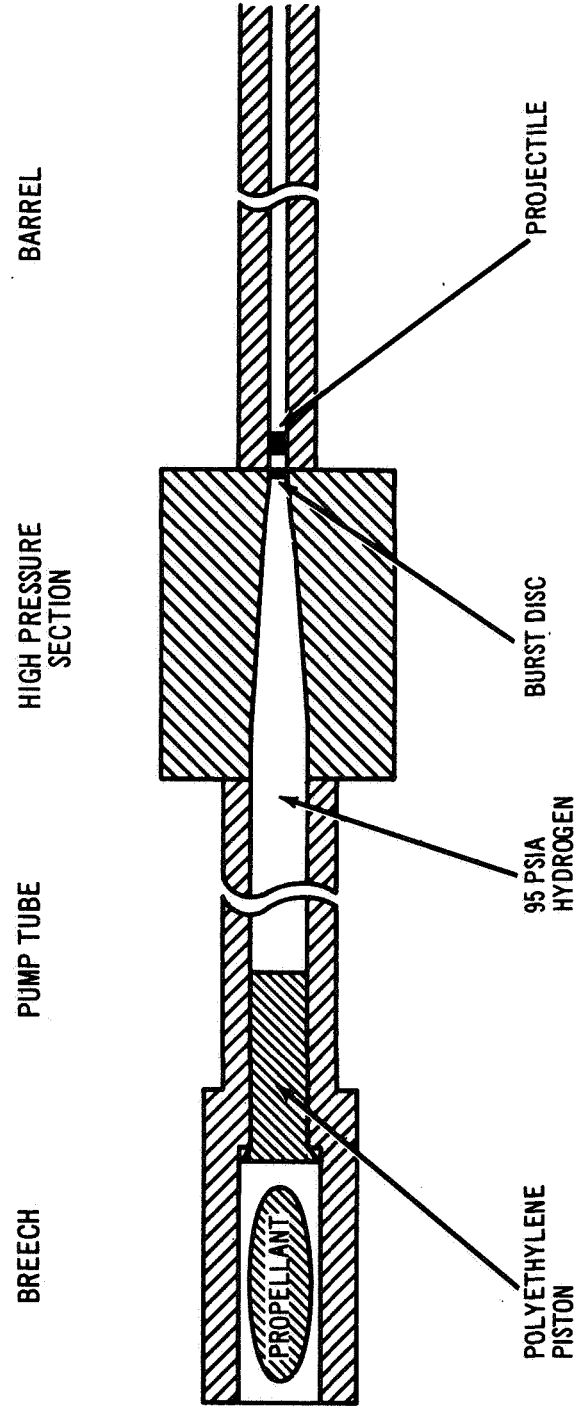


FIGURE 4. SCHEMATIC DIAGRAM OF BASIC  
LIGHT GAS GUN

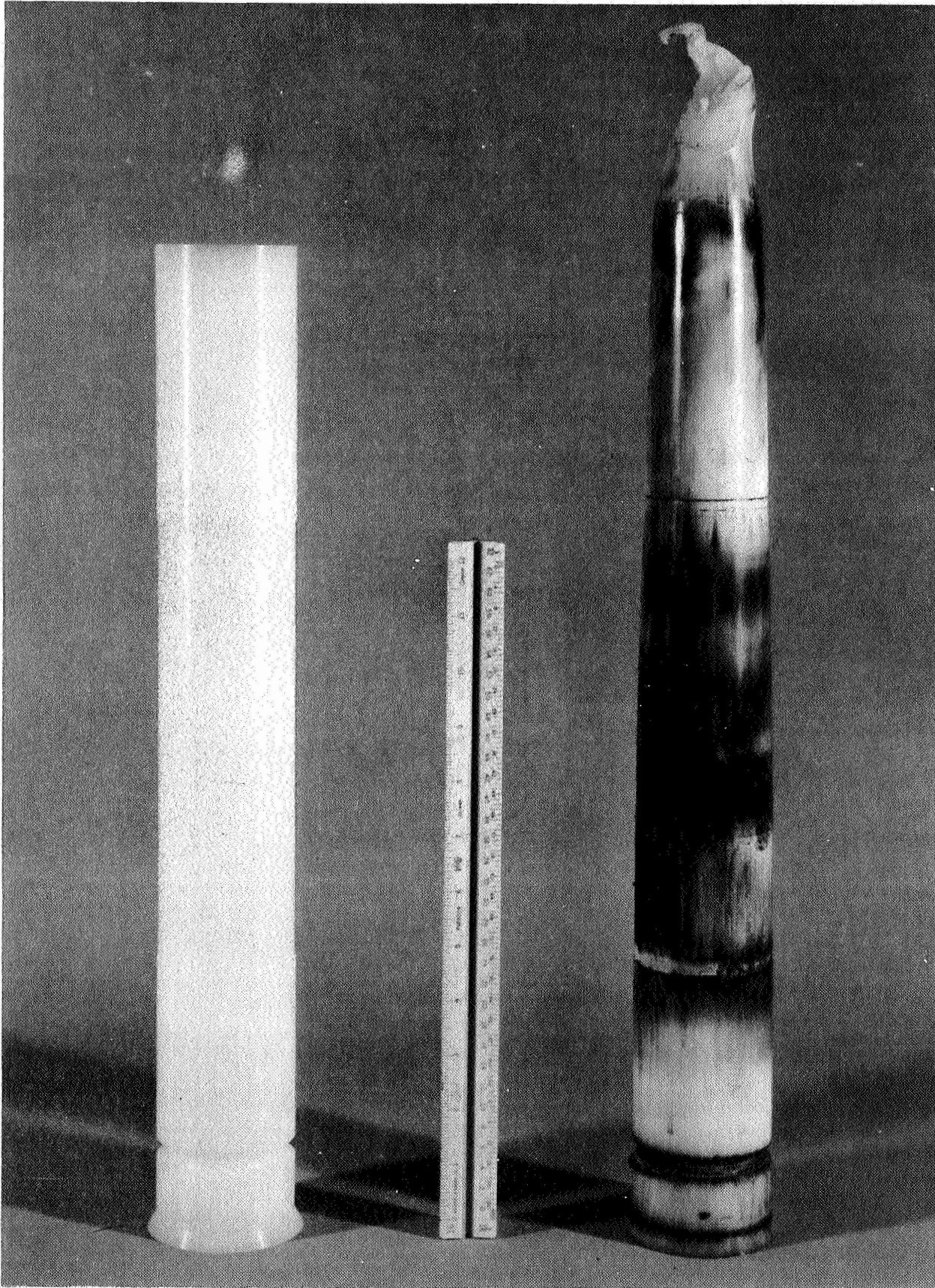


FIGURE 5. POLYETHYLENE PISTON BEFORE  
AND AFTER FIRING

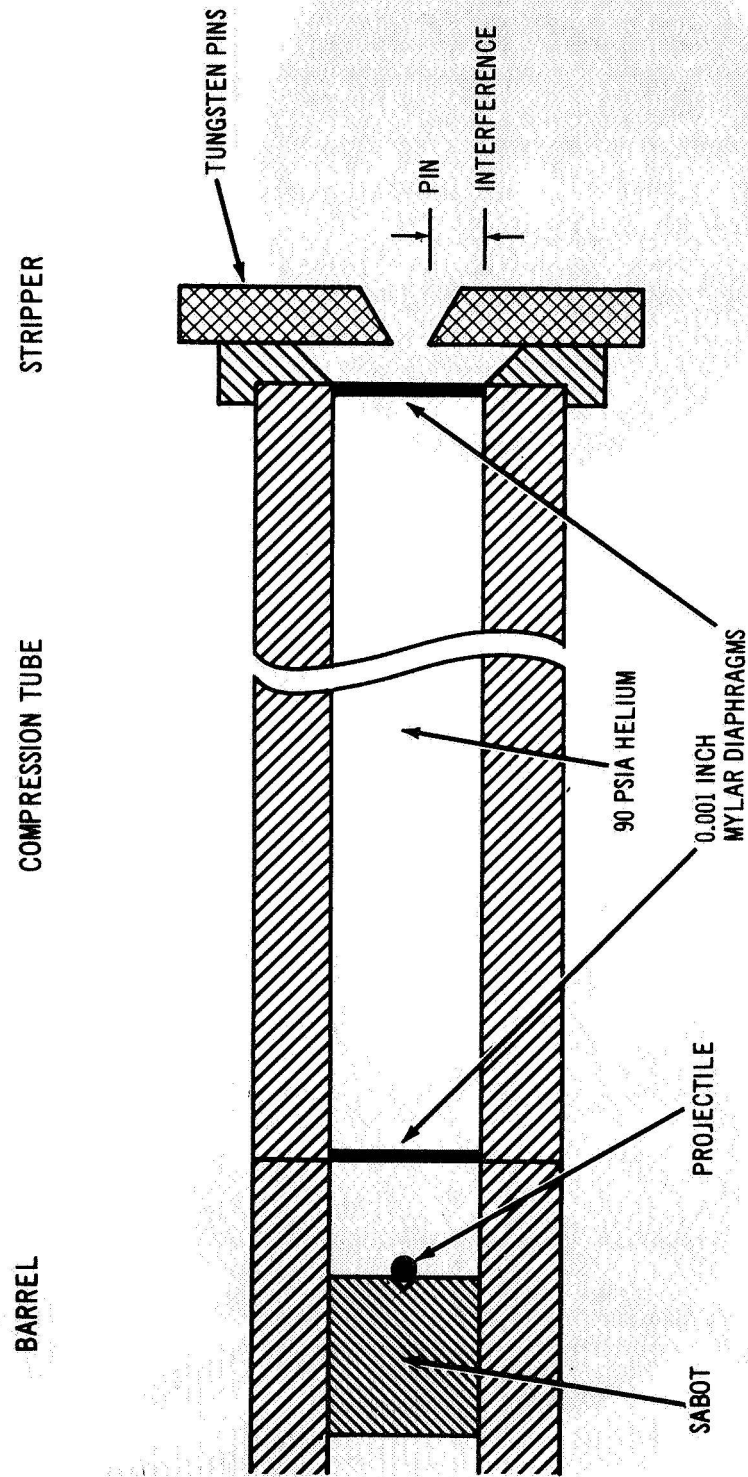


FIGURE 6. SCHEMATIC DIAGRAM OF SABOT STRIPPER AND GAS SEPARATOR TUBE

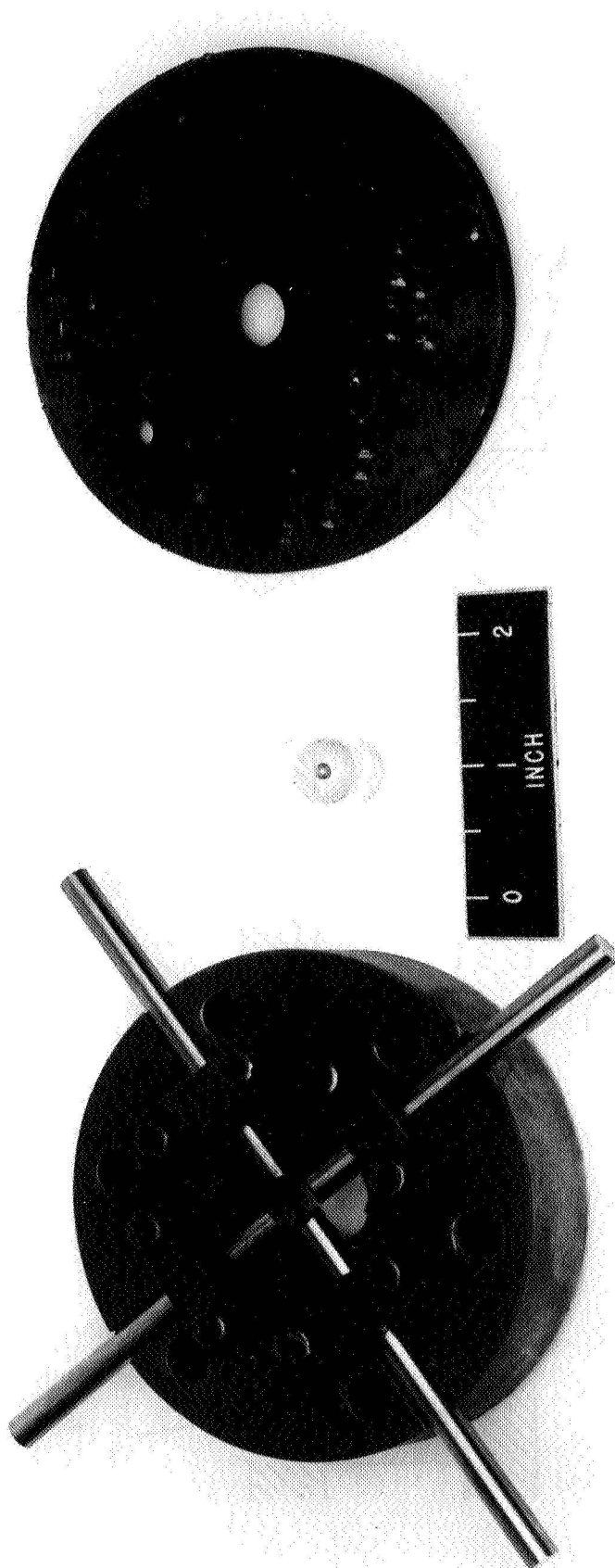


FIGURE 7. STRIPPER PIN ASSEMBLY, SABOT WITH PROJECTILE, AND SABOT TRAP

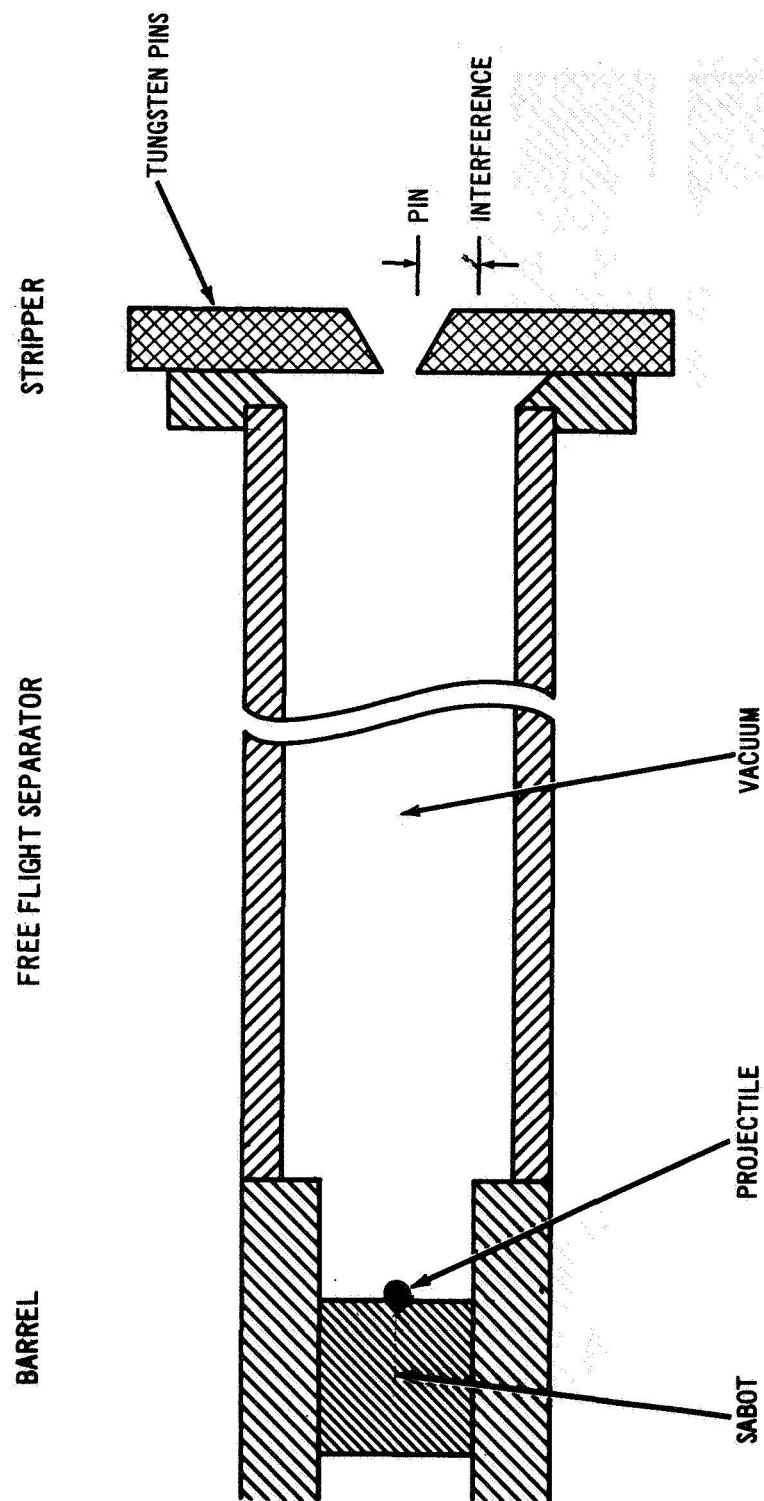


FIGURE 8. SCHEMATIC DIAGRAM OF SABOT STRIPPER AND FREE FLIGHT SEPARATOR

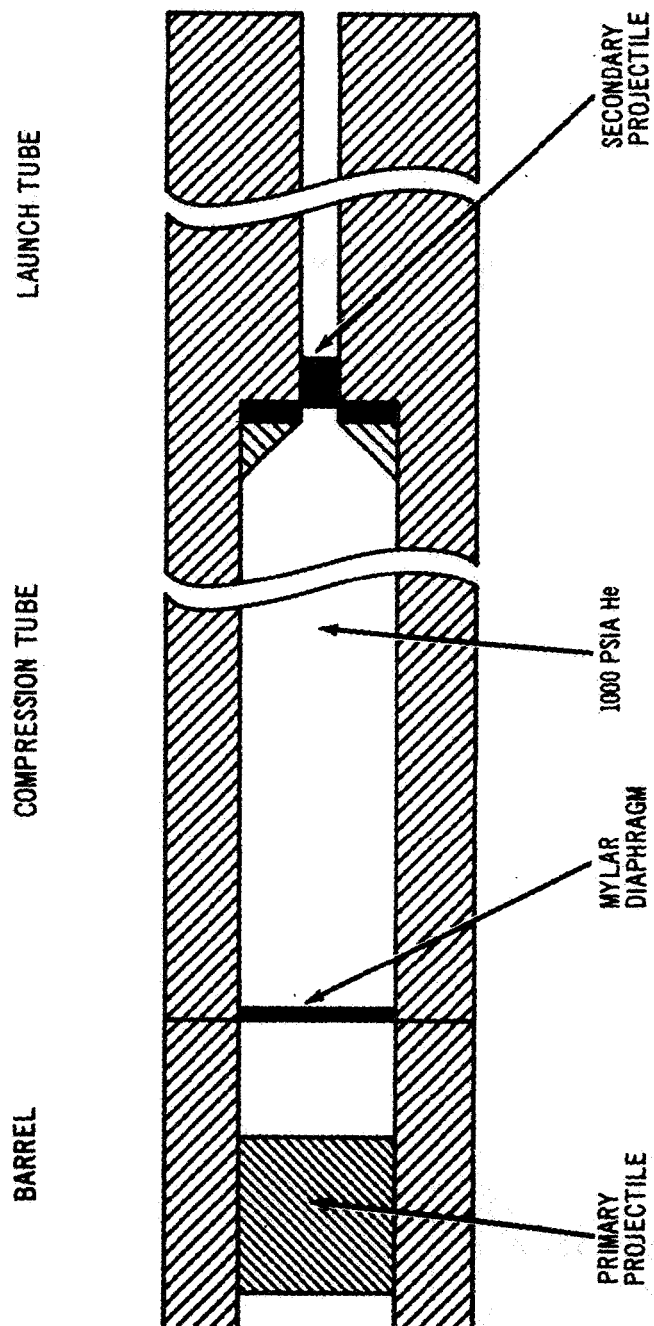


FIGURE 9. SCHEMATIC DIAGRAM OF  
REDUCED AREA ACCELERATOR

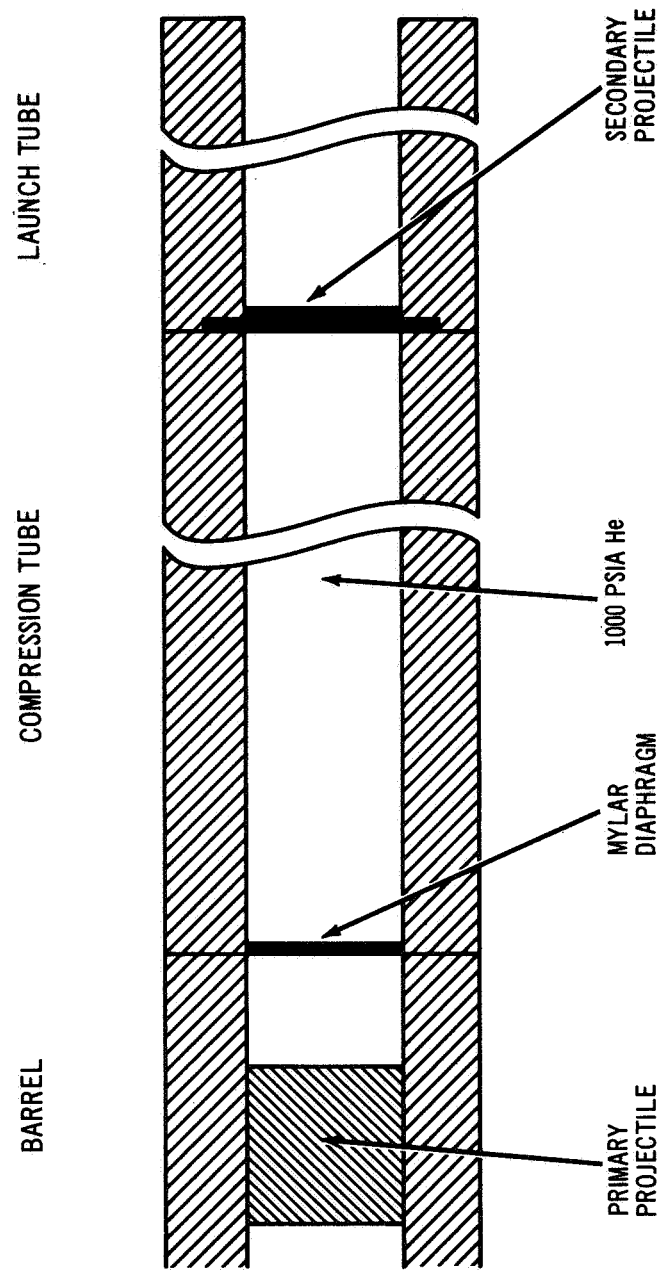


FIGURE 10. SCHEMATIC DIAGRAM OF  
CONSTANT AREA ACCELERATOR

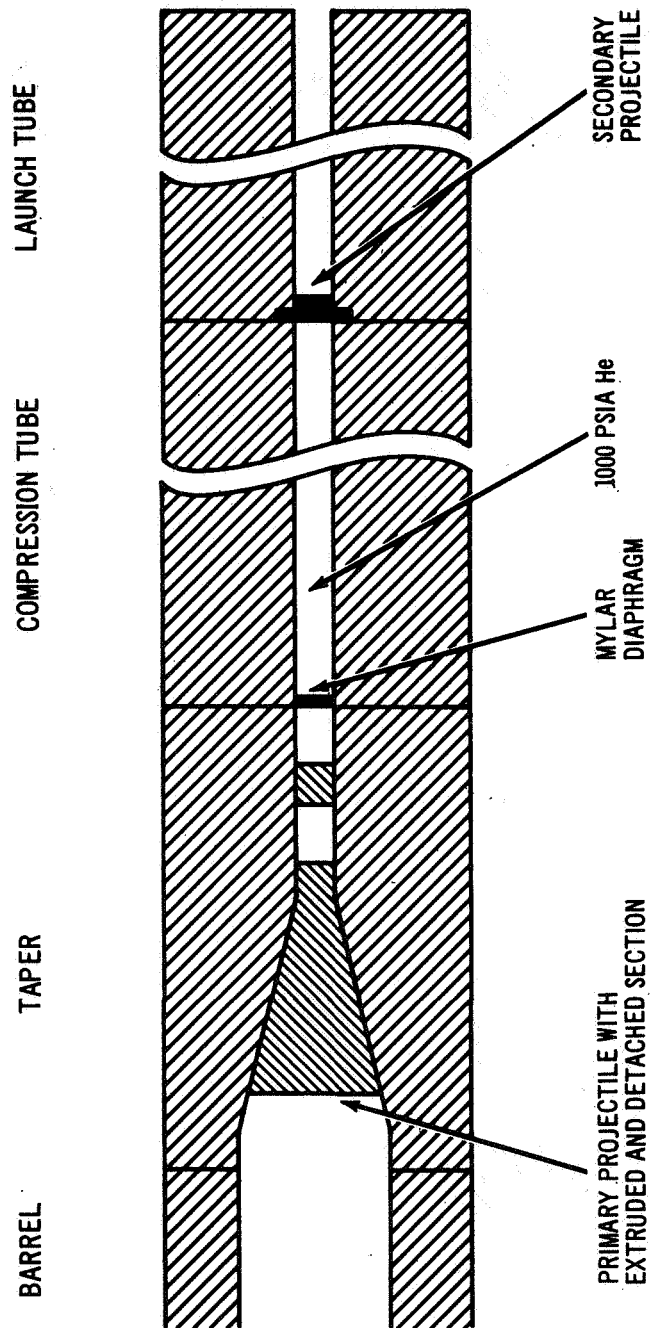


FIGURE 11. SCHEMATIC DIAGRAM OF TAPERED  
ENTRANCE ACCELERATOR

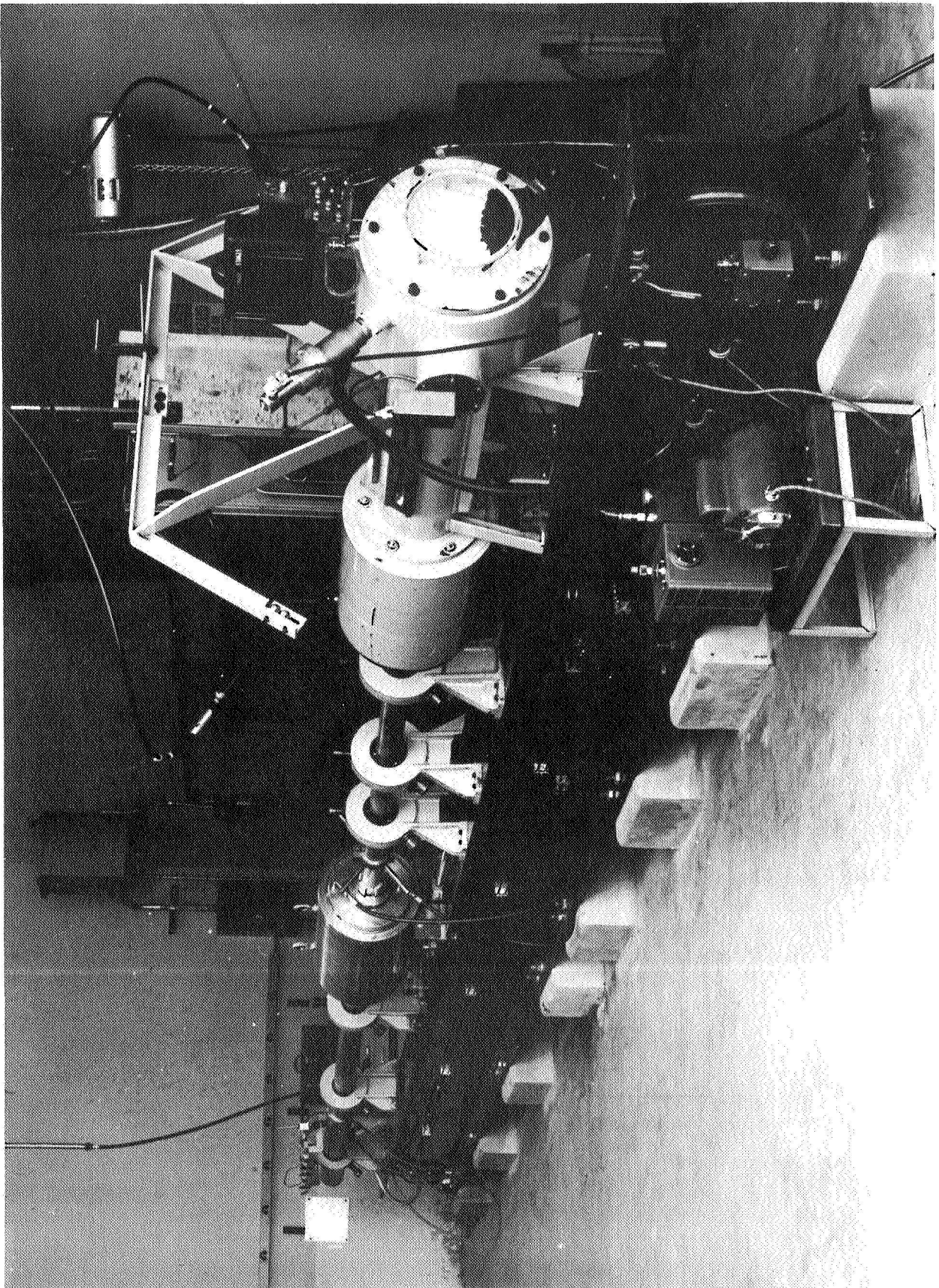


FIGURE 12. RANGE TANK OF METEOROID  
SIMULATION FACILITY

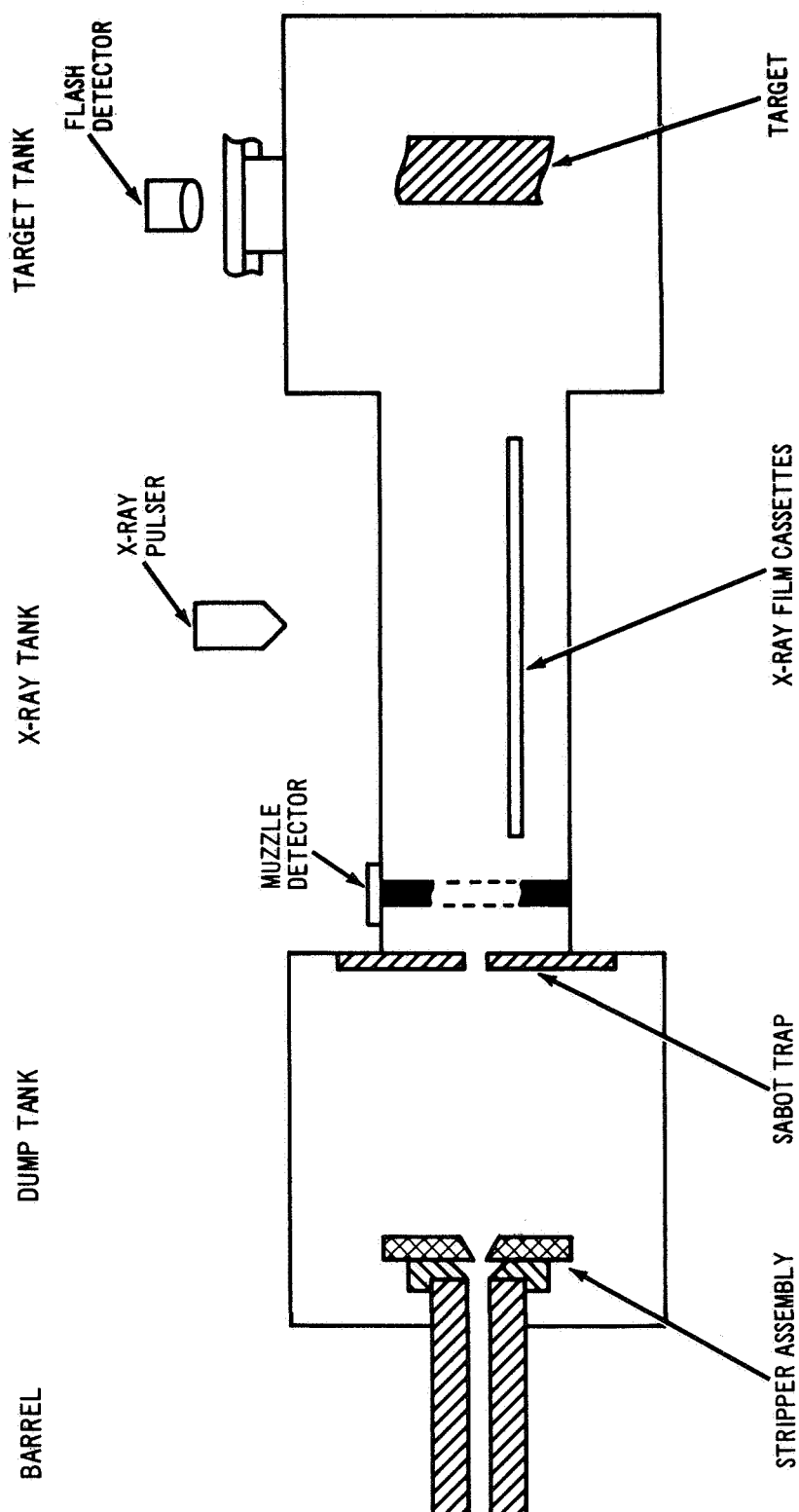


FIGURE 13. SCHEMATIC DIAGRAM OF  
RANGE TANK

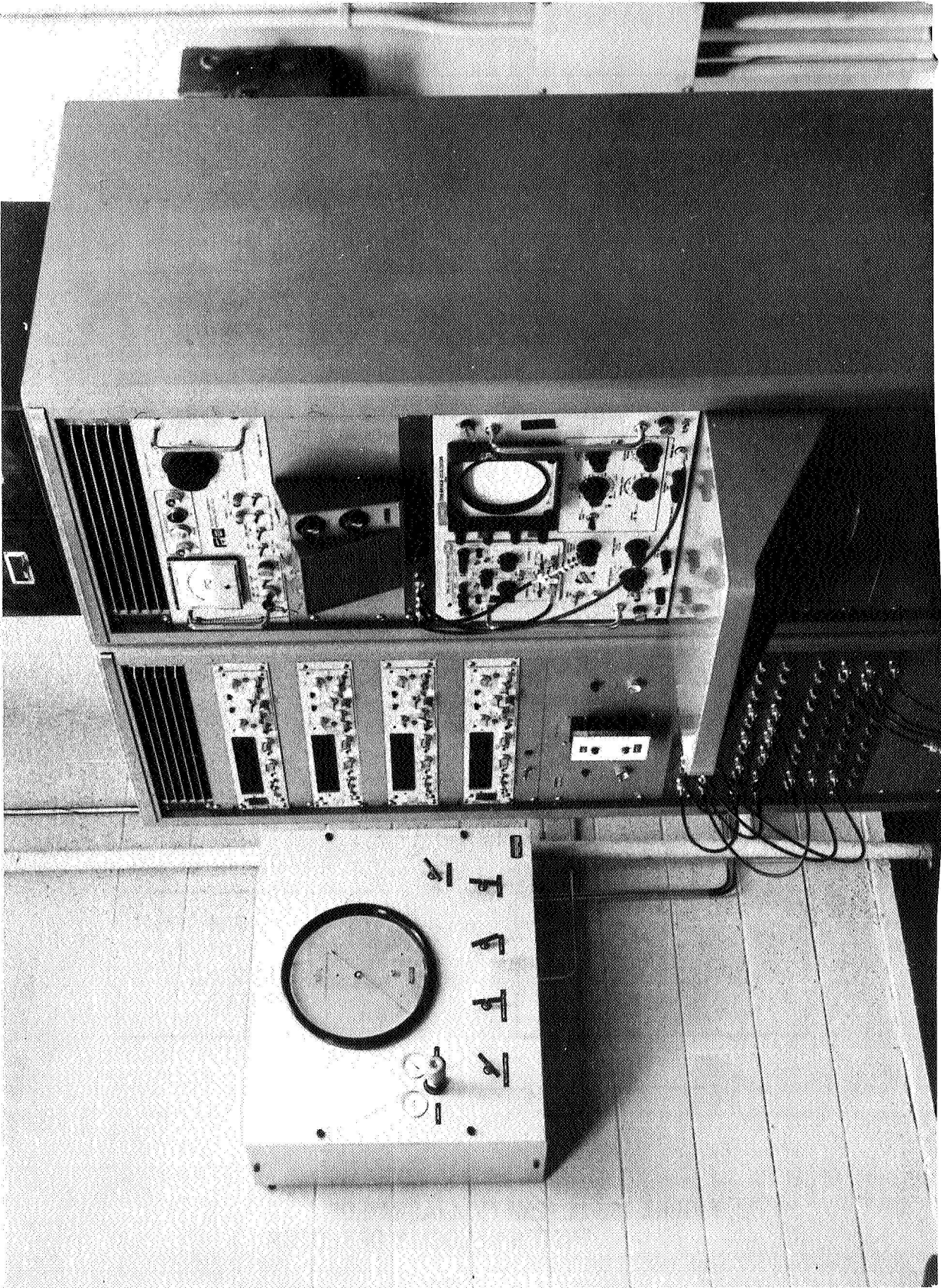


FIGURE 14. CUNIKUL KUUM INSTRUMENTATION

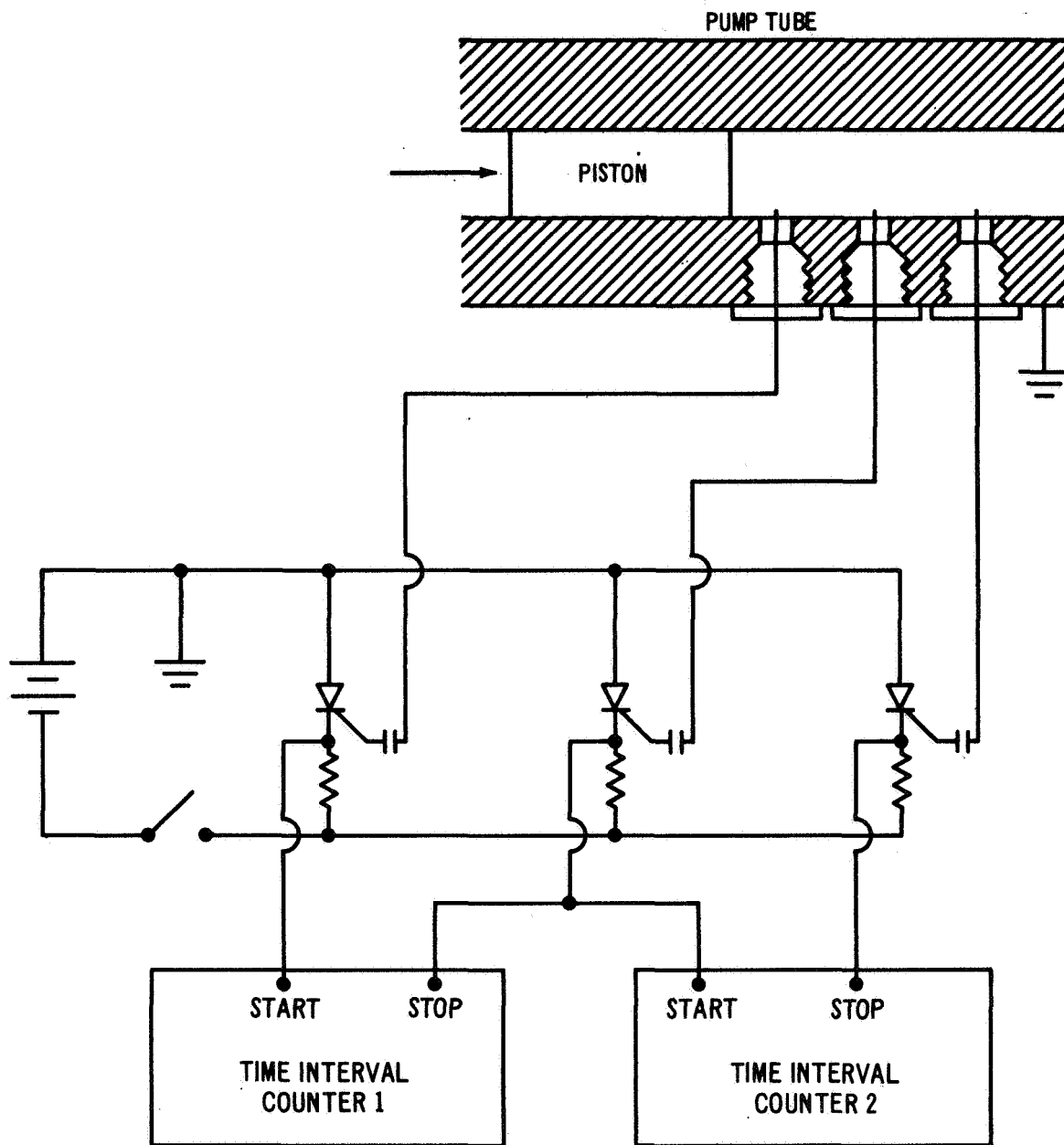


FIGURE 15. SCHEMATIC DIAGRAM OF  
PISTON VELOCITY DETECTOR

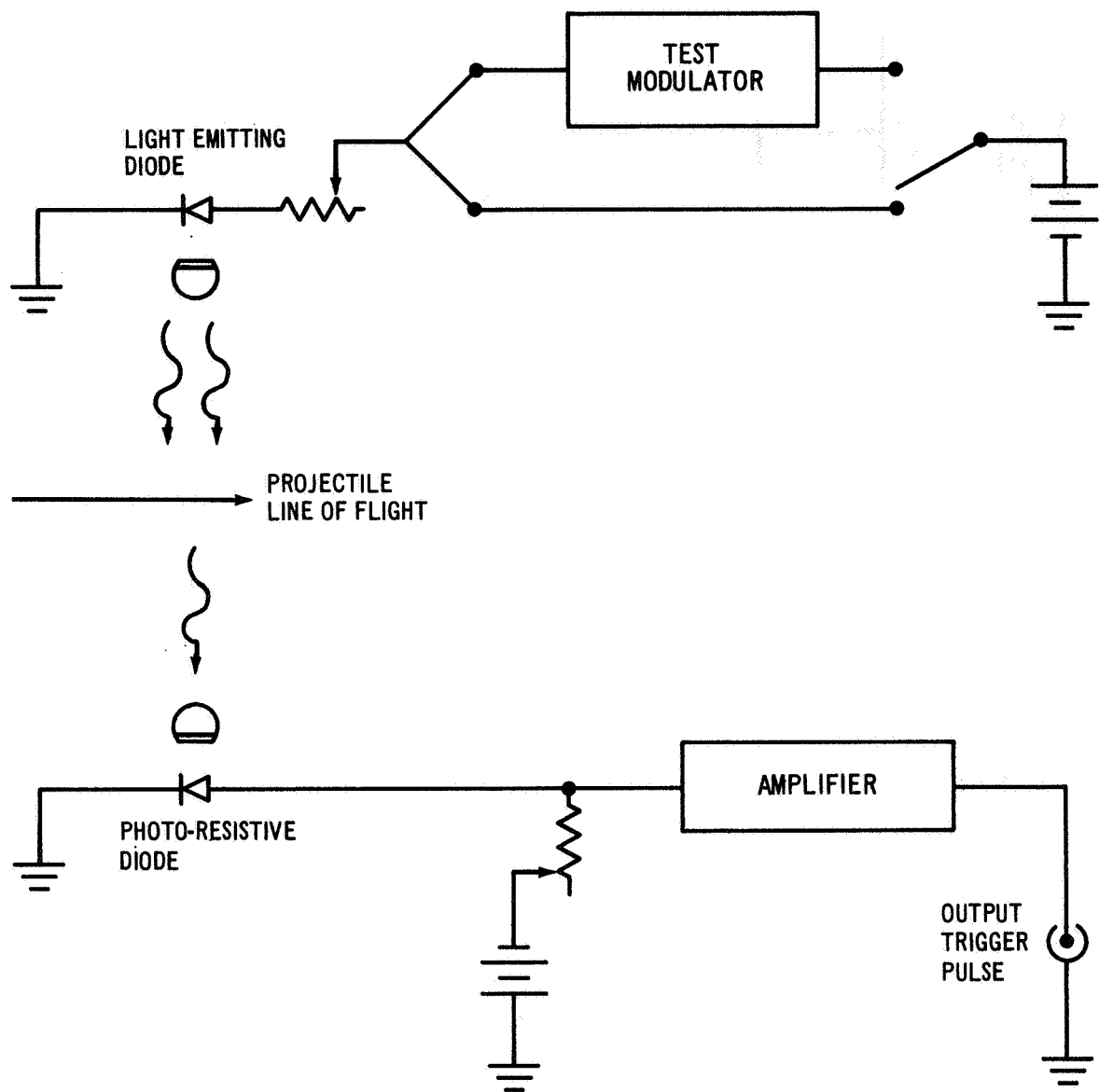


FIGURE 16. BLOCK DIAGRAM  
OF MUZZLE DETECTOR

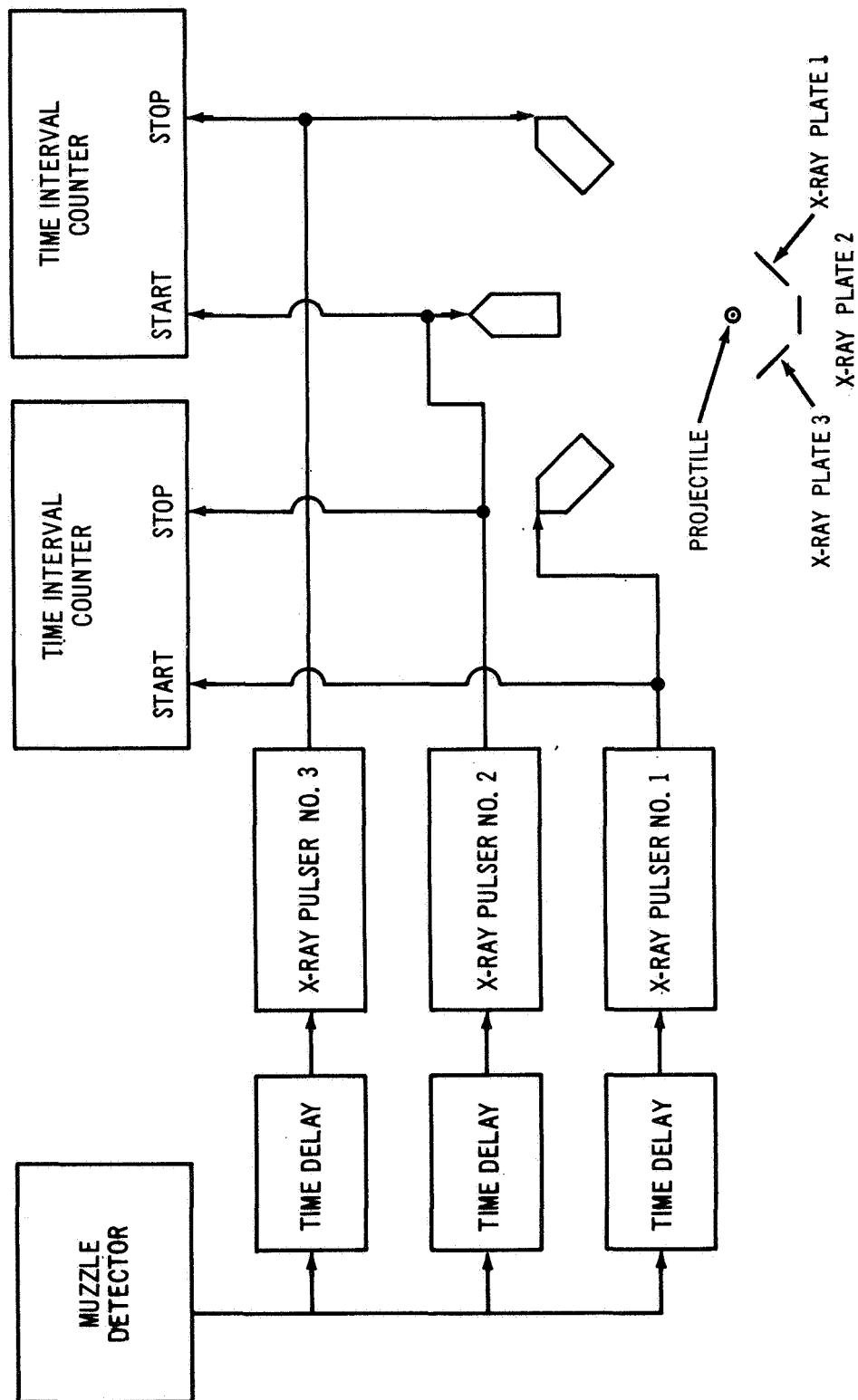


FIGURE 17. BLOCK DIAGRAM OF THE PROJECTILE  
VELOCITY DETECTOR

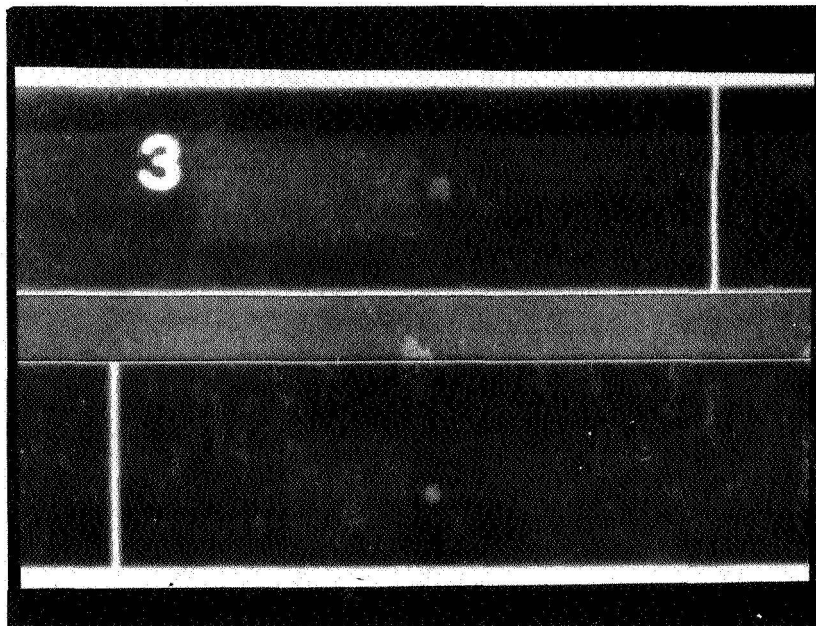


FIGURE 18. X-RAY IMAGES OF TWO TYPES OF  
SABOT AND PROJECTILE CONFIGURATIONS

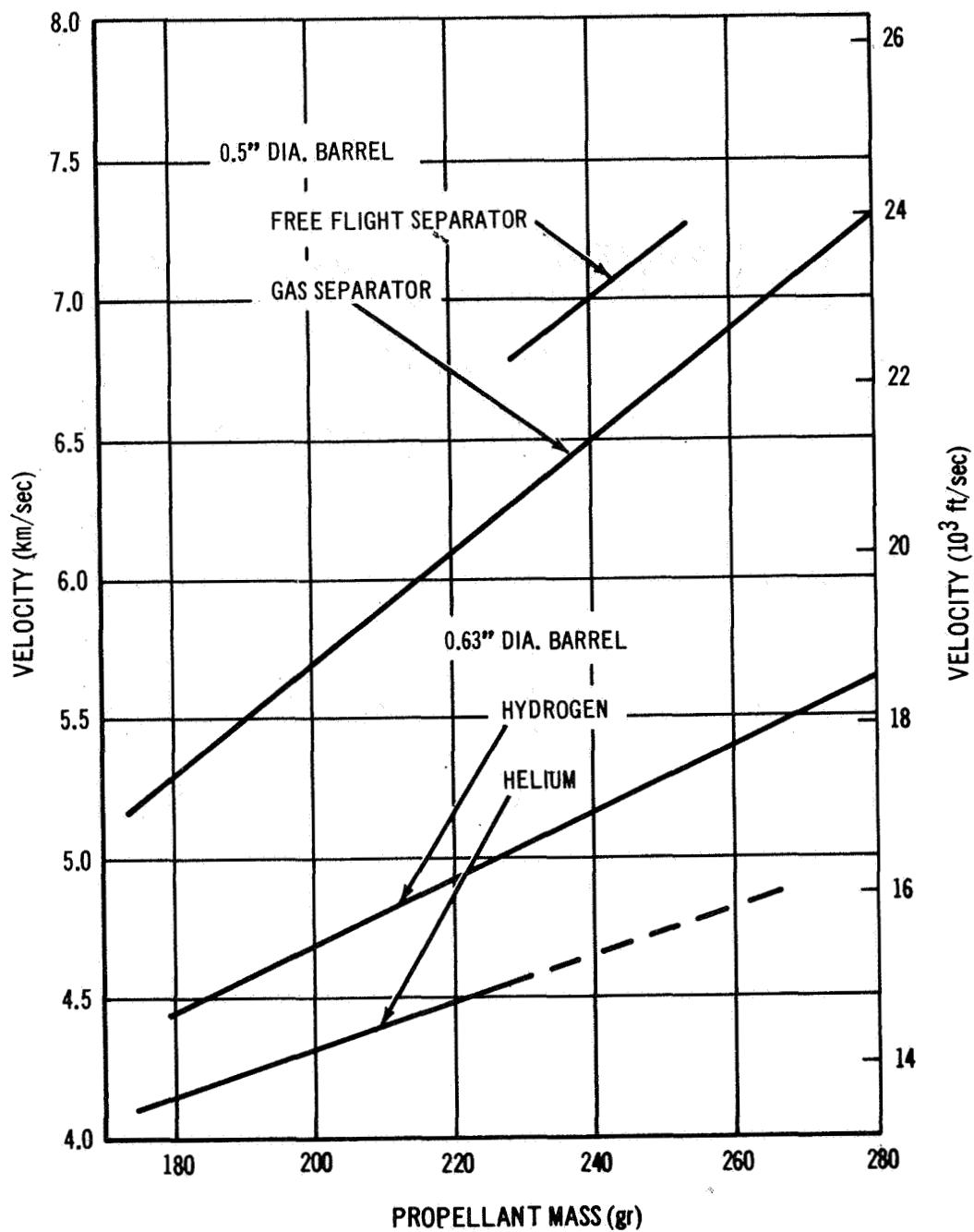


FIGURE 19. PROPELLANT MASS VS. VELOCITY  
FOR SPECIFIC LAUNCHING PARAMETERS

FRONT

PROJECTILE: 4 GRAM LEXAN  
VELOCITY: 5.10 km/sec  
(16,700 ft/sec)

BACK

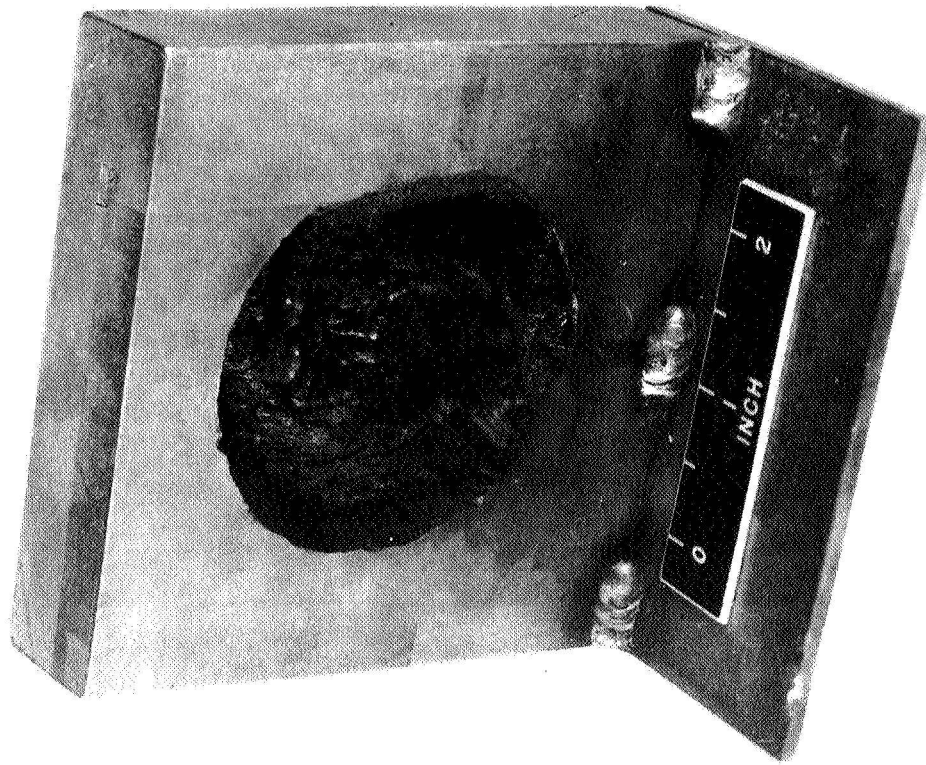
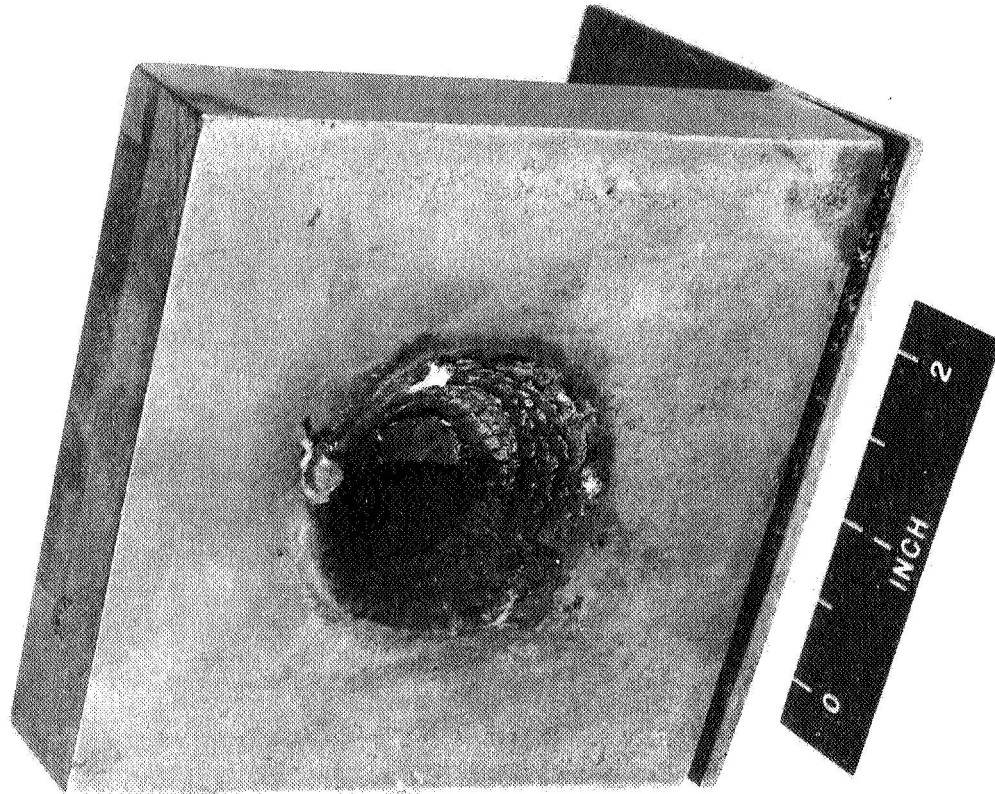


FIGURE 20. TARGET USED IN SHOT 24  
SHOWING CRATER AND SPALL

PROJECTILE: 4 GRAM LEXAN

VELOCITY: 4.31 km/sec  
(14,100 ft/sec)

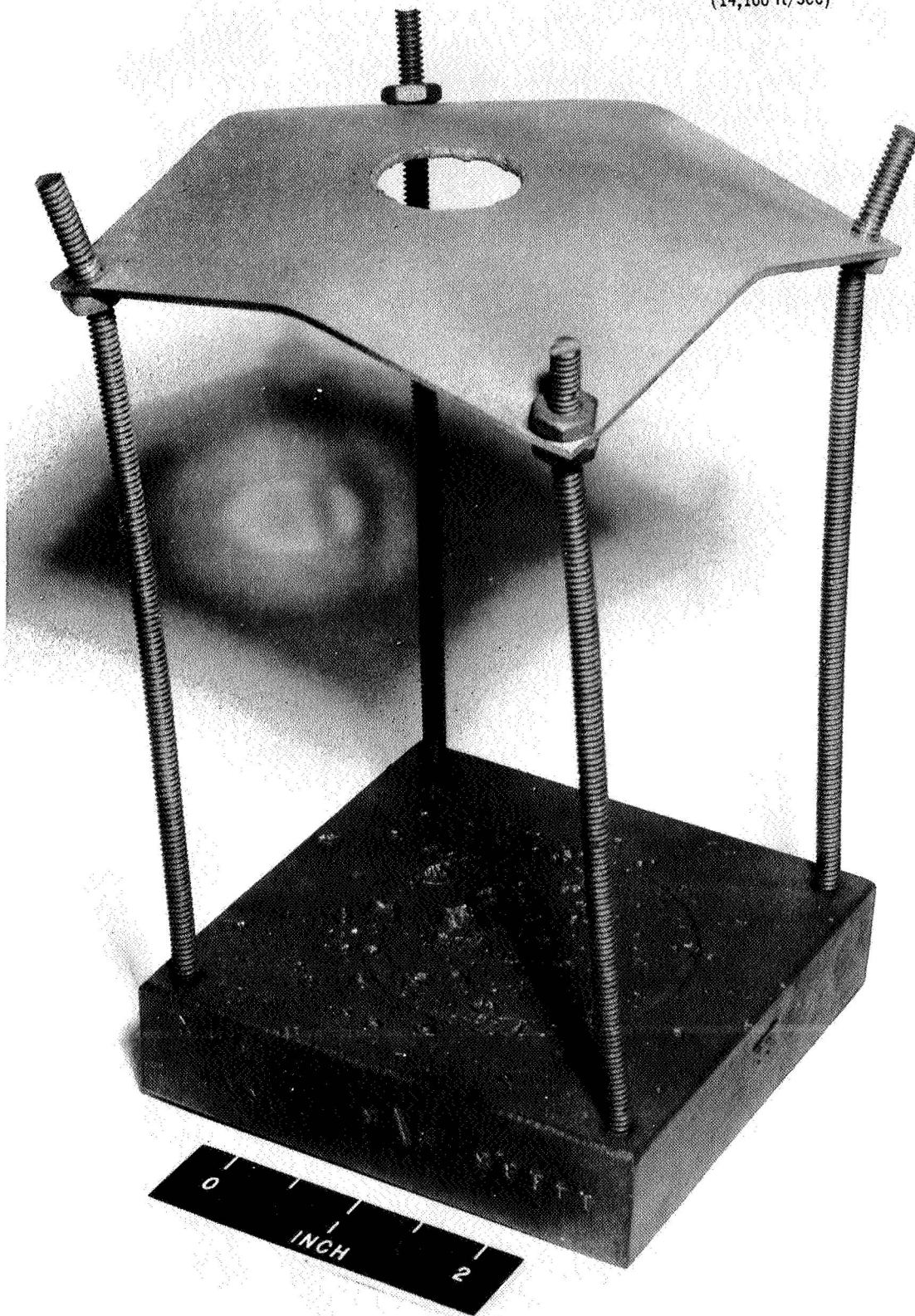


FIGURE 21. TARGET USED IN SHOT 11 SHOWING  
CIRCULAR SYMMETRY PRODUCED  
BY BUMPER IMPACT

PROJECTILE: 0.047 GRAM AL. SPHERE  
VELOCITY: 6.75 km/sec  
(22,100 ft/sec)

TARGET: 1.0 INCH AL.  
BUMPER: 0.012 INCH AL.  
SEPARATION: 2.36 INCH

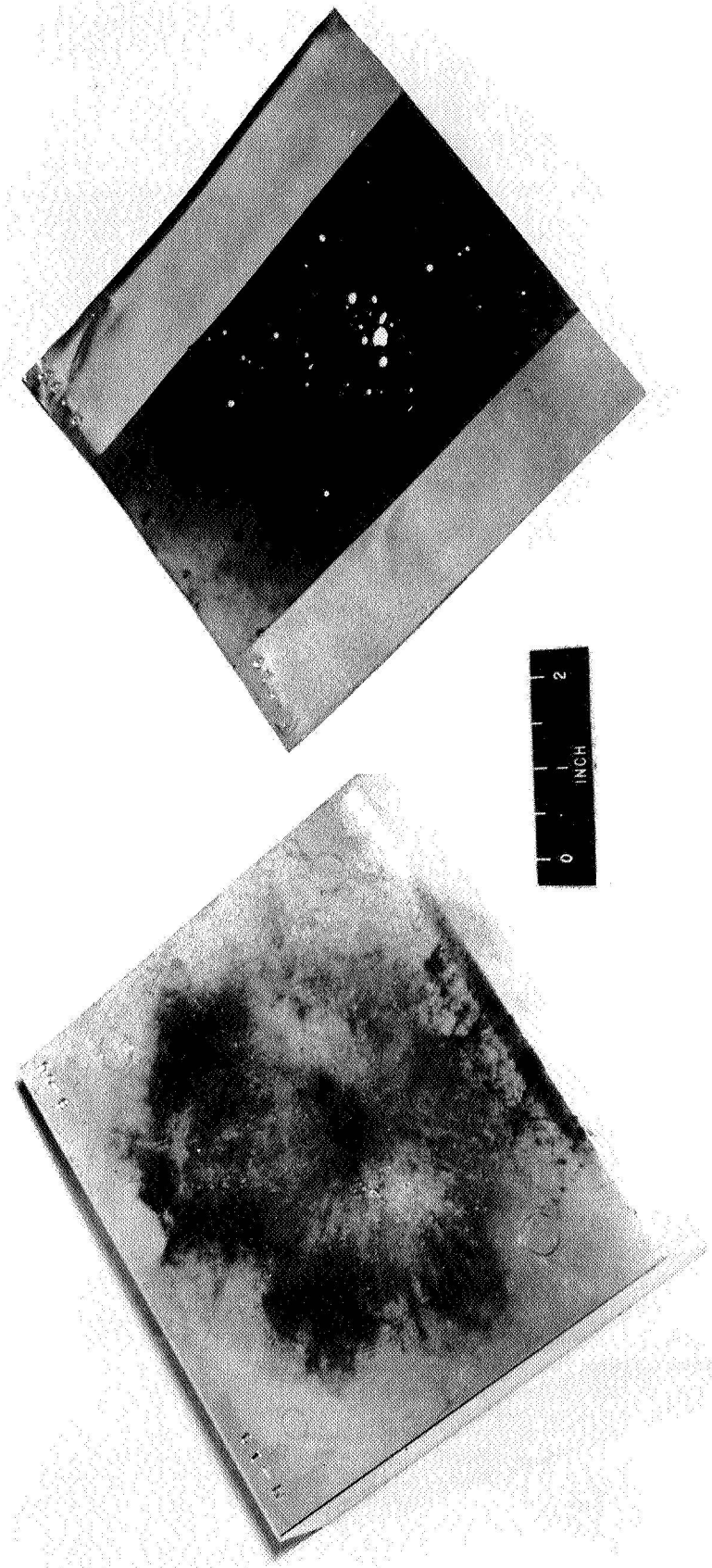


FIGURE 22. TARGET AND BUMPER USED IN  
SHOT 55

TARGET: 1.0 INCH AL.  
BUMPER: 0.012 INCH AL.  
SEPARATION: 2.36 INCH

PROJECTILE: 0.047 GRAM AL. SPHERE  
VELOCITY: 6.58 km/sec  
(21,600 ft/sec)

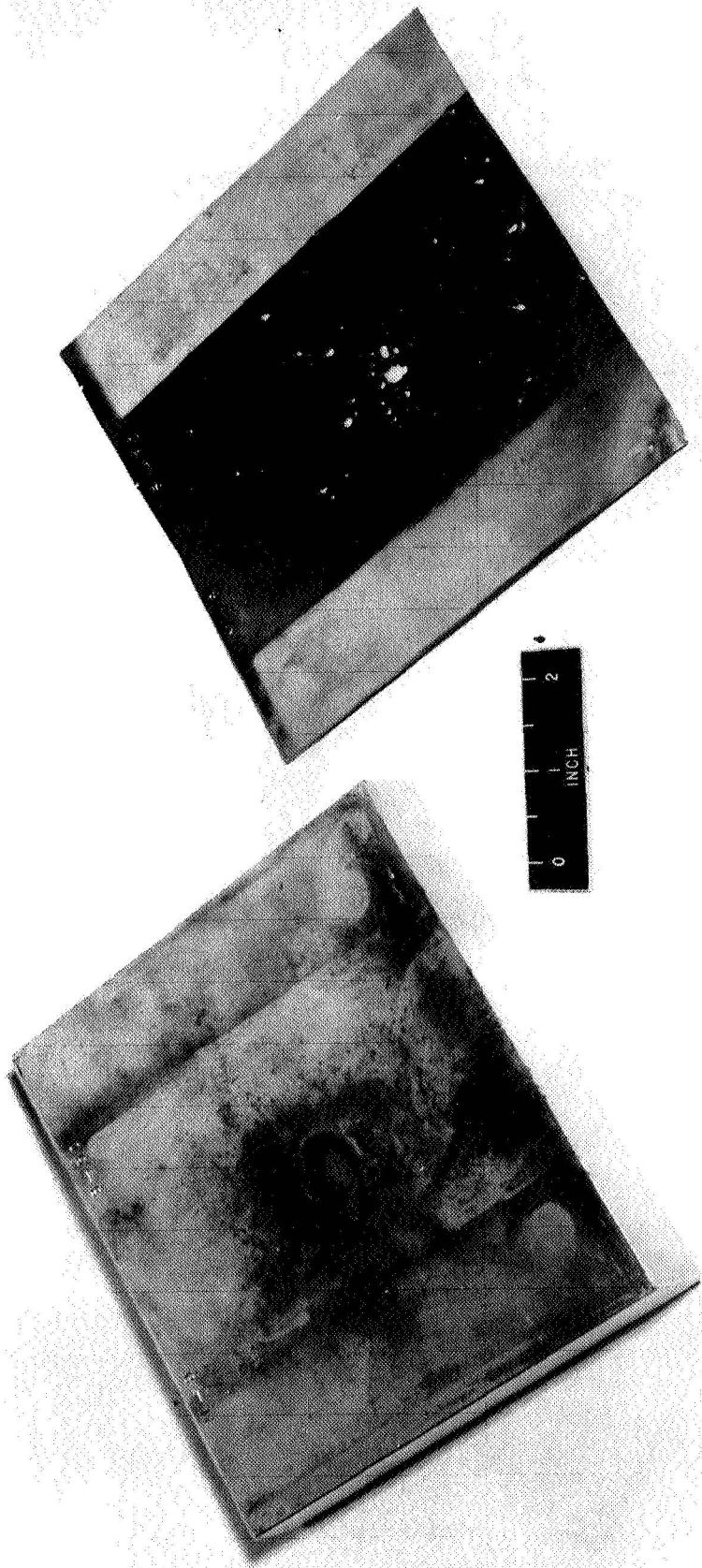


FIGURE 23. TARGET AND BUMPER USED IN  
SHOT 50 INDICATING DEBRIS  
LEADS PROJECTILE

#### REFERENCES

1. Dalton, Charles C.: Meteoroid Flux and Puncture Models for Cislunar Space, NASA TM X-53507, 1965.
2. Dalton, Charles C.: Near Earth and Interplanetary Meteoroid Flux and Puncture Models, Memorandum R-AERO-Y-160-67, February 20, 1967.
3. Proceedings of the Seventh Hypervelocity Impact Symposium, Vol. VI, Martin Company, Orlando, Florida (Symposium Coordinator), February 1965.
4. Explosive Hypervelocity Launcher, Contract Number NAS2-3577, Ames Research Center.
5. Development of a Micrometeoroid Simulation Device, Vol. I, Final Report, Contract Number NAS8-20529, Marshall Space Flight Center.
6. Development of a Micrometeoroid Simulation Device, Volume II, Final Report, Contract Number NAS8-20529, Marshall Space Flight Center.
7. Kottenstette, James P. and Howell, William G.: Development and Analysis of a Third Stage Accelerator for a Light Gas Gun, Proceedings of the Seventh Hypervelocity Impact Symposium, Volume I, Page 45, Martin Company, Orlando, Florida (Symposium Coordinator), February 1965.

September 26, 1968

APPROVAL

TM X-53787


DEVELOPMENT OF THE MATERIALS DIVISION METEOROID SIMULATION FACILITY

By

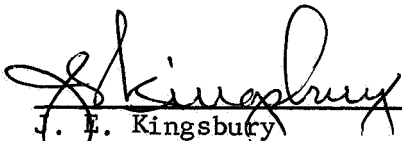
R. C. Ruff

The information in this report has been reviewed for security classification. Review of any information concerning Department of Defense or Atomic Energy Commission programs has been made by the MSFC Security Classification Officer. This report, in its entirety, has been determined to be unclassified.

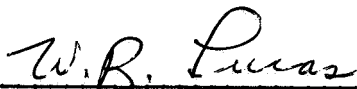
This document has also been reviewed and approved for technical accuracy.



E. C. McKannan  
Chief, Engineering Physics Branch



J. E. Kingsbury  
Chief, Materials Division



W. R. Lucas  
Director, Propulsion and Vehicle Engineering  
Laboratory

September 26, 1968

TM X-53787

DISTRIBUTION

DIR	Dr. von Braun
DEP-T	Dr. Rees
R-DIR	Mr. Weidner
R-AERO-DIR	Dr. Geissler
R-AERO-P	Mr. Sims
R-AS-DIR	Mr. Williams
R-ASTR-DIR	Dr. Haeussermann
R-ASTR-BA	Mr. Thornton
R-COMP-DIR	Dr. Hoelzer
R-COMP-RR	Mr. Tondera
R-ME-DIR	Mr. Kuers
R-ME-A	Mr. Crumpton
R-OM-DIR	Colonel Fellows
R-OM-V	Mr. Cash
R-QUAL-DIR	Mr. Grau
R-QUAL-J	Mr. Henning
R-SE-DIR	Mr. Richard
R-SE-V	Mr. Collins
R-SSL-DIR	Dr. Stuhlinger
R-SSL-SF	Mr. Duncan
R-SSL-PM	Mr. Naumann
R-TEST-DIR	Mr. Heimbürg
R-TEST-B	Mr. Hamilton
R-P&VE-DIR	Dr. Lucas
R-P&VE-E	Mr. Brooksbank
R-P&VE-M	Mr. Kingsbury (6)
R-P&VE-MC	Mr. Nunnelley
R-P&VE-M	Mr. Riehl
R-P&VE-ME	Mr. McKannan (5)
R-P&VE-MEV	Mr. Ruff (20)
R-P&VE-MM	Mr. Cataldo
R-P&VE-MN	Mr. Curry
R-P&VE-M	Mr. Gray
R-P&VE-M	Mr. Holmes
R-P&VE-M	Mr. Zoller
R-P&VE-P	Mr. Paul
R-P&VE-RM	Mr. Locke
R-P&VE-S	Mr. Kroll
R-P&VE-SAA	Mr. Nevins (5)
R-P&VE-V	Mr. Aberg
R-P&VE-X	Mr. McCool
R-P&VE-XAW	Mr. Roach
I-DIR	General O'Connor
I-DIR	Dr. Mrazek

September 26, 1968

NASA TM X-53787

DISTRIBUTION (Concluded)

I-RM-M	Mr. Goldston
I-S/AA-MGR	Mr. Belew
I-S/AA	Mr. Field
I-S/AA	Mr. Ferguson
I-S/AA	Mr. Waite
MS-IP	Mr. Ziak
MS-IL	Miss Robertson (8)
MS-H	Mr. Akens
PAT	Mr. Rice
MS-T	Mr. Wiggins (6)

Scientific and Technical Information Facility (25)  
P. O. Box 33  
College Park, Maryland 20740